AD

USAAVLABS TECHNICAL REPORT 67-43

EVALUATION OF TWO TITANIUM FORGING ALLOYS

By

Charles J. Matusovich

August 1967

U. S. ARMY AVIATION MATERIEL LABORATORIES
FORT EUSTIS, VIRGINIA

CONTRACT DA 44-177-AMC-256(T)

SIKORSKY AIRCRAFT
DIVISION OF UNITED AIRCRAFT CORPORATION
STRATFORD, CONNECTICUT

89

Disclaimers

When Government drawings, specifications, or other data are used for any purpose other than in connection with a definitely related Government procurement operation, the United States Government thereby incurs no responsibility nor any obligation whatsoever; and the fact that the Government may have formulated, furnished, or in any way supplied the said drawings, specifications, or other data is not to be regarded by implication or otherwise as in any manner licensing the holder or any other person or corporation, or conveying any rights or permission, to manufacture, use, or sell any patented invention that may in any way be related thereto.

Trade names cited in this report do not constitute an official endorsement or approval of the use of such commercial hardware or software.

Disposition Instructions

Destroy this report when no longer needed. Do not return it to originator.

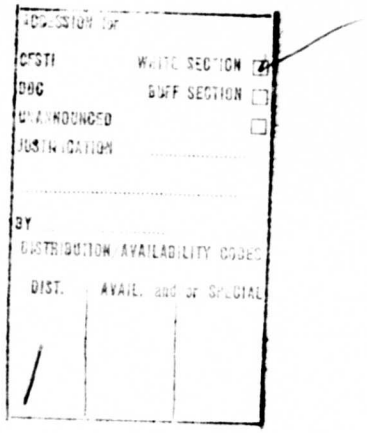

DEPARTMENT OF THE ARMY
U. S. ARMY AVIATION MATERIEL LABORATORIES
FORT EUSTIS, VIRGINIA 23604

This program was carried out under Contract DA 44-177-AMC-256(T) with Sikorsky Aircraft Division of United Aircraft Corporation.

The data contained in this report are the results of research conducted on titanium forging alloys to determine their fatigue properties. Two promising titanium forging alloys (Ti-6Al-2Sn and Ti-13V-11Cr-3Al) were considered.

The report has been reviewed by the U. S. Army Aviation Materiel Laboratories and is considered to be technically sound. It is published for the exchange of information and the stimulation of future research.

Task 1F121401A14176
Contract DA 44-177-AMC-256(T)
USAAVLABS Technical Report 67-43
August 1967

EVALUATION OF TWO TITANIUM FORGING ALLOYS

Sikorsky Engineering Report SER-50430

By

Charles J. Matusovich

Prepared by

Sikorsky Aircraft Division of United Aircraft Corporation
Stratford, Connecticut

for

U. S. ARMY AVIATION MATERIEL LABORATORIES
FORT EUSTIS, VIRGINIA

ABSTRACT

Two titanium forging alloys have been evaluated for aerospace applications: (a) Ti-6Al-6V-2Sn and (b) Ti-13V-11Cr-3Al (both solution heat-treated and aged). Both small-size specimens and full-size helicopter components were tested.

The small-size specimens were tested for resistance to fatigue crack initiation, resistance to fatigue crack propagation, and fracture toughness. Fatigue crack initiation tests included tension-tension tests both of unnotched specimens and of joints. Helicopter main rotor cuffs were evaluated in fatigue crack initiation and fatigue crack propagation tests with expanded holes and with reamed holes. The titanium alloy cuff test results were compared to those for Ti-6Al-4V (annealed) and 4340 steel (heat-treated to a 125-ksi minimum ultimate tensile strength) cuffs and to small-size specimen tests. Tensile test data, chemical analysis and forging parameters are also presented.

The crack initiation resistance of Ti-6Al-6V-2Sn was found to be superior to that of Ti-13V-11Cr-3Al. Axial tension-tension fatigue results showed 50% higher fatigue strengths for Ti-6Al-6V-2Sn than for Ti-13V-11Cr-3Al. Joint fatigue tests also showed higher strength values for the Ti-6Al-6V-2Sn alloy. Fracture toughness results were comparable for both alloys.

Joint fatigue test evaluations were made for reamed, shot peened, and expanded holes. The highest fatigue strength values were associated with specimens having expanded holes.

The Ti-6Al-6V-2Sn cuffs with both reamed and expanded cuff-to-spar attachment holes showed higher fatigue crack initiation strength values than those of the Ti-13V-11Cr-3Al.

The Ti-6Al-6V-2Sn cuffs showed higher resistance to crack propagation than Ti-13V-11Cr-3Al, with both reamed and expanded holes, and were comparable in resistance to crack propagation with 4340 steel and Ti-6Al-4V shot peened.

FOREWORD

This report is submitted in accordance with United States Army Aviation Materiel Laboratories Contract DA 44-177-AMC-256(T), Evaluation of Two Titanium Forging Alloys. Research was conducted from May 1965 to January 1967 in the contractor's test facilities located at

Sikorsky Aircraft Division of United Aircraft Corporation
Main Street
Stratford, Connecticut

The following personnel were directly associated with this research program:

Administrative Task Coordinator - William G. Degnan
Technical Task Coordinator for Small-Size Specimen Testing and Metallurgy - Leonard Robins
Technical Task Coordinator for Cuff Testing - Walter A. Lane
Test Engineer - Henry M. Borowy
Test Engineer - Joseph P. Franko
Test Engineer - Charles J. Matusovich

Acknowledgement is given to the following for the cooperation freely given to make this program a success: J. J. Zecco, Jr., and R. E. Sparks of Wyman-Gordon Company, forging subcontractor; W. H. Heil of Titanium Metals Corporation, material supplier; and J. H. Milo of Metal Improvement Company, shot peening vendor.

BLANK PAGE

CONTENTS

ILLUSTRATIONS

TABLES

SYMBOLS

The following symbols are used throughout the report:

E	modulus of elasticity
π	constant, equal to 3.141
psi	pounds per square inch
ksi	thousands of pounds per square inch
°F	degrees Fahrenheit

The following symbols are primarily associated with fatigue crack initiation tests:

S_V	vibratory stress in fatigue curve shape equation, $$S_V = E_S + \frac{\alpha}{N^\gamma}$$
E_S	estimated endurance strength at an infinite number of cycles (used in the fatigue curve shape equation)
E_T	sample mean endurance strength at an infinite number of cycles
N	number of cycles of applied vibratory load
α	evaluated constant in the fatigue curve shape equation
γ	evaluated constant in the fatigue curve shape equation
$\bar{X}$	sample arithmetic mean
s	sample standard deviation
$s/\bar{X}$	sample coefficient of variation

The following symbols are associated with fatigue crack propagation and fracture toughness tests:

2a	fatigue crack length (natural fatigue crack in fatigue crack propagation and fracture toughness specimens)

2b, w	width of specimen
v	vertical displacement of two points (1 inch above and 1 inch below a crack under static load) as measured with a compliance gage
S_g	gross stress across uncracked cross-sectional area of fatigue crack propagation or fracture toughness specimens
K	stress intensity factor (psi $\sqrt{\text{inch}}$) of elastic stress field in the vicinity of the crack tip
K_{Ic}	critical stress intensity factor associated with initiation of unstable plane-strain fracturing (stress intensity factor needed to start a crack propagating under a static load)
K_c	critical stress intensity factor associated with initiation of unstable plane-stress fracture (stress intensity factor needed to produce an unstable crack under a static load)
G	energy to propagate a crack (inch-pounds per inch) or strain-energy release rate as the crack extends
G_{Ic}	critical crack extension force associated with initiation on unstable plane-strain fracturing
G_c	critical crack extension force associated with initiation of unstable plane-stress fracturing

The following symbols are primarily associated with (static) tensile tests:

e	elongation (tensile) in a 2-inch gage length
R.A.	reduction in area
F_{tu}	ultimate tensile strength
F_{ty}	0.2% offset tensile yield strength
μ	Poisson's ratio, unit lateral contraction divided by unit longitudinal elongation

The following symbols are associated with graphical illustrations throughout the report:

O	indicates data point for small-size specimen tests

▽ indicates data point in Figures 15 and 18 for specimen failure originating in hole processed with roller burnishing tool

◹ indicates data point in Figures 15 and 18 for specimen failure originating in hole processed with bearingizing tool

▽→ indicates data point for specimen "run out" in Figures 15 and 18

◇ indicates data point for Ti-6Al-6V-2Sn cuff with expanded holes

◊ indicates data point for Ti-13V-11Cr-3Al cuff with expanded holes

◇ indicates data point for Ti-6Al-6V-2Sn cuff with reamed holes

□ indicates data point for Ti-13V-11Cr-3Al cuff with reamed holes

⌂ indicates data point for Ti-6Al-4V cuff with shot peened holes

⬡ indicates data point for 4340 steel cuffs with reamed holes

INTRODUCTION

Aerospace applications constantly demand the greatest strength-to-weight ratio available in materials. Interest in two titanium forging alloys, Ti-6Al-6V-2Sn and Ti-13V-11Cr-3Al, is based on the high strength-to-weight ratio attainable in the tensile properties of these alloys in the heat-treated condition. Additional factors which cause interest in these alloys are the good formability and the attainment of uniform, high mechanical properties throughout heavy sections.

These two alloys represent the most promising of two separate families of titanium alloys. The Ti-6Al-6V-2Sn is one of a series of alpha-beta alloys based on the original and highly successful Ti-6Al-4V. The Ti-13V-11Cr-3Al is an all-beta alloy which has shown good mechanical properties throughout heavy sections.

This research evaluation concerns only fatigue properties and support data for fatigue properties. General mechanical property data existed for these alloys, but specific information on fatigue properties, particularly as affected by production surface conditions, was lacking. Finally, fatigue crack initiation and propagation data for a full-size structure produced by current forging practices were desired for these forging alloys.

In organizing this report, procedure, results, and discussion of results have been reviewed separately for each of the mechanical properties evaluated. A list of the mechanical properties evaluated is given below.

1. Fatigue crack initiation strength in shot peened open sections.

2. Fatigue crack initiation strength in joints with reamed, shot peened, and expanded hole surfaces. (NOTE: Stress concentration factors of joint geometry and fretting corrosion are combined in this test series.)

3. Fatigue crack propagation strength in shot peened open sections.

4. Fracture toughness.

5. Full-size component fatigue crack initiation and propagation strengths and comparison of full-size component results and small-specimen results.

Supporting information, such as tensile properties, chemical analyses, forging, and heat-treating variables, has been presented in the appendix.

SECTION I - AXIAL TENSION-TENSION FATIGUE TESTS

EXPERIMENTAL PROCEDURE

Three forgings of each alloy were cut into specimen blanks and identified as shown in Figure 1. The blanks were machined to the required dimensions shown in Figure 2. The reduced section of the specimen shown in Figure 2 was shot peened with S-110 shot to a 6A intensity. Specimen identification was retained throughout all processing operations.

With the specimen identification and a table of random numbers, the specimens were arranged in a random manner from the three forgings. Eighteen specimens were obtained from each forging and were listed. Groups of specimens were chosen from this list and were assigned to specific stress levels. From this same list, without reference to stress level, the specimens were scheduled for testing on the six fatigue machines, described below, using the same randomization technique. Finally, the completed schedule was examined to assure that no anomalies in the randomization had occurred. Typical of the anomalies considered was that a large portion of the specimens from one forging might have been scheduled to be tested on the same fatigue machine. No anomalies of this type were found.

The constant load fatigue machines with five-to-one amplifiers, Sonntag Scientific Corporation, Model SF-1-U, are shown in Figure 3. In this figure (right, center) is also an Ellis Company Model BA-12 bridge amplifier and a cathode ray oscilloscope which was used to measure the applied loads.

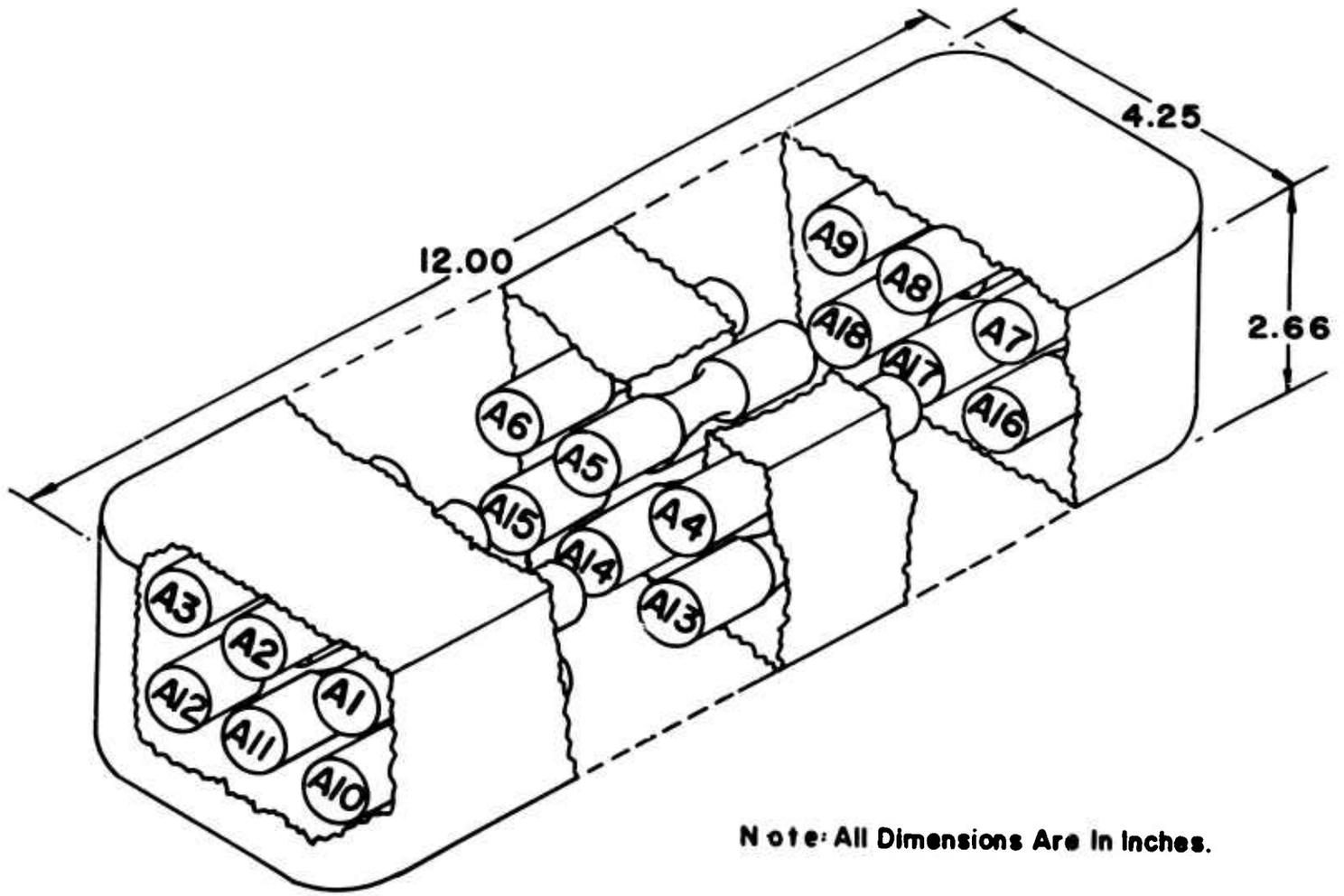

Figure 1. Location of Axial Tension-Tension Fatigue Specimens in Forging.

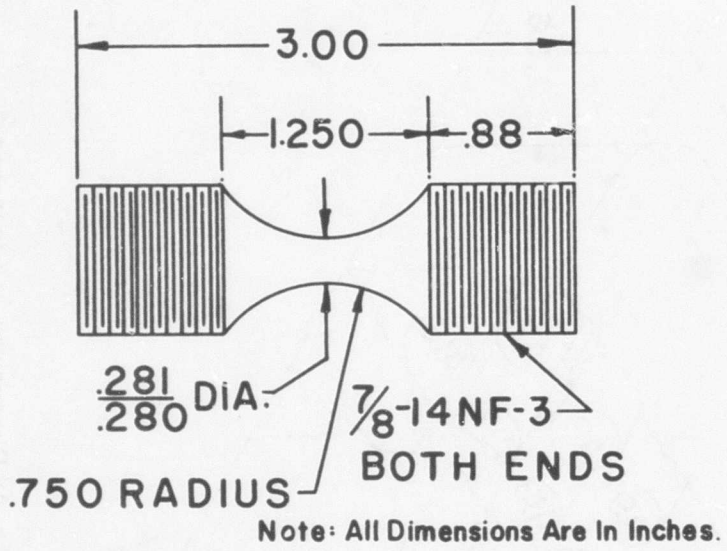

Figure 2. Dimensioned Sketch of Axial Tension-Tension Fatigue Specimen.

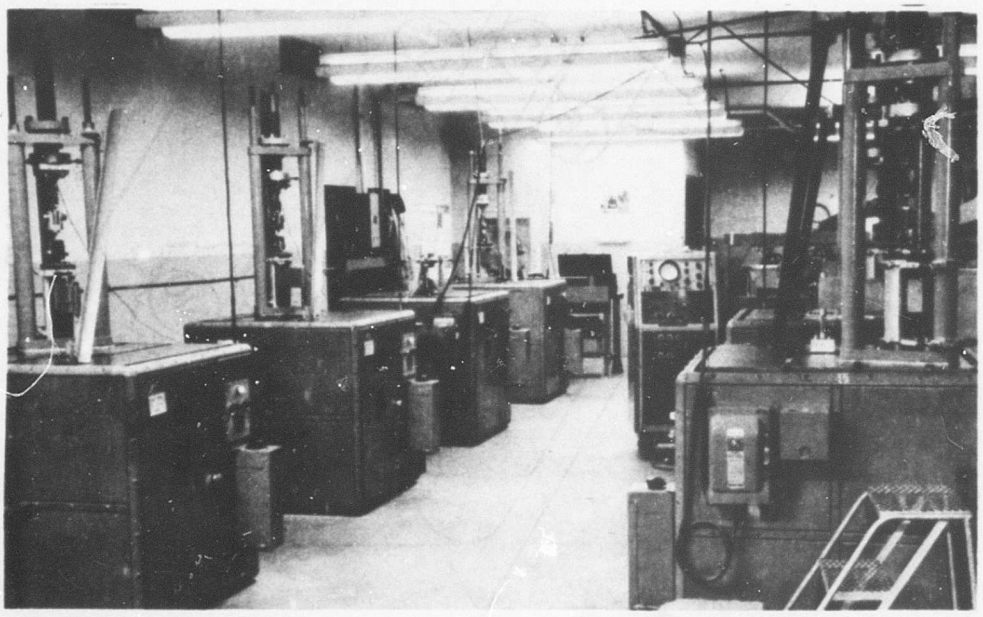

Figure 3. General Facilities of Applied Research Laboratory.

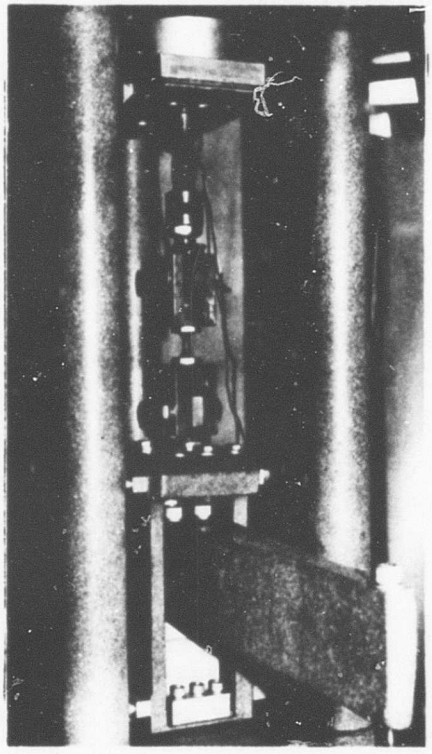

Figure 4. Axial Specimen Installed in SF-1-U Five-to-One Amplifier.

Figure 4 shows a specimen installed in series with a load cell in the five-to-one amplifying fixture on a constant-load fatigue machine. Each load cell was calibrated statically in a Riehle PS-60 tensile machine; the Ellis BA-12 bridge amplifier and oscilloscope were used to read the load cell strain gage bridge output. The calibrated load cell was used to read the static and dynamic loads applied to each specimen. The estimated accuracy for load measurements is ± 2%. The overall testing accuracy for true stress measurement is estimated to be approximately ± 4% including the potential inherent bending stresses due to eccentricity of loading.

The axial fatigue data were analyzed statistically, and parameters were determined as follows. At each test level (example: + 70,000 ± 60,000 psi) the logarithmic mean (i.e., arithmetic mean of the logarithm of the cycles to failure) was determined. A best-fitting smooth curve was drawn through these logarithmic mean points. Coordinate points of the mean curve and E_S, the estimated mean endurance strength at an infinite number of cycles, were substituted into a curve shape equation of the form

$$S_V = E_S + \frac{\alpha}{N^{\gamma}}$$

and the constants of the equation (α and γ) were determined.

The IBM 7094 digital computer located in United Aircraft Research Laboratories, East Hartford, Connecticut, was used in processing the individual test failure point coordinates, the equation stated above, and the constants of that equation. The computer calculated the sample standard deviation, the sample mean endurance strength at an infinite number of cycles, E_T, and the sample coefficient of variation. The computer also

calculated specific stress and cycle intercepts of the mean curve. These values were used to draw mean curves shown in this report.

EXPERIMENTAL RESULTS AND DISCUSSION OF RESULTS

A minimum of 30 specimens of each alloy were tested with mean stress (70,000 psi) held constant to produce the S/N curves shown in Figures 5 and 6. In analyzing the fatigue data, the results shown in Table I were obtained.

TABLE I

AXIAL TENSION-TENSION FATIGUE TEST RESULTS

Alloy	E_T (psi)	α	γ	s (psi)*	$\bar{X}$ (psi)*	$s/\bar{X}$ (%)*
Ti-6Al-6V-2Sn	14,900	37,000	.20	1640	29,500	5.6
Ti-13V-11Cr-3Al	16,000	17,000	.35	1680	19,400	8.6

*Applicable at 10^8 cycles of vibratory stress.

Comparison of the mean strength and the coefficient of variation at 10^8 cycles shows the higher strength of Ti-6Al-6V-2Sn over Ti-13V-11Cr-3Al.

It should be noted that the equations whose constants are listed in Table I above are based on results in the range of from 10^5 to 10^8 cycles. Beyond 10^8 cycles or at less than 10^5 cycles, the equations should be used with caution, since no test data were obtained in these regions.

Figures 7 and 8 shown typical fatigue fracture surfaces of the two alloys in the high cycle (above 10^6) portion of the S/N curve. Subsurface origins are evident due to the compressive stresses induced in the specimen surface by shot peening.

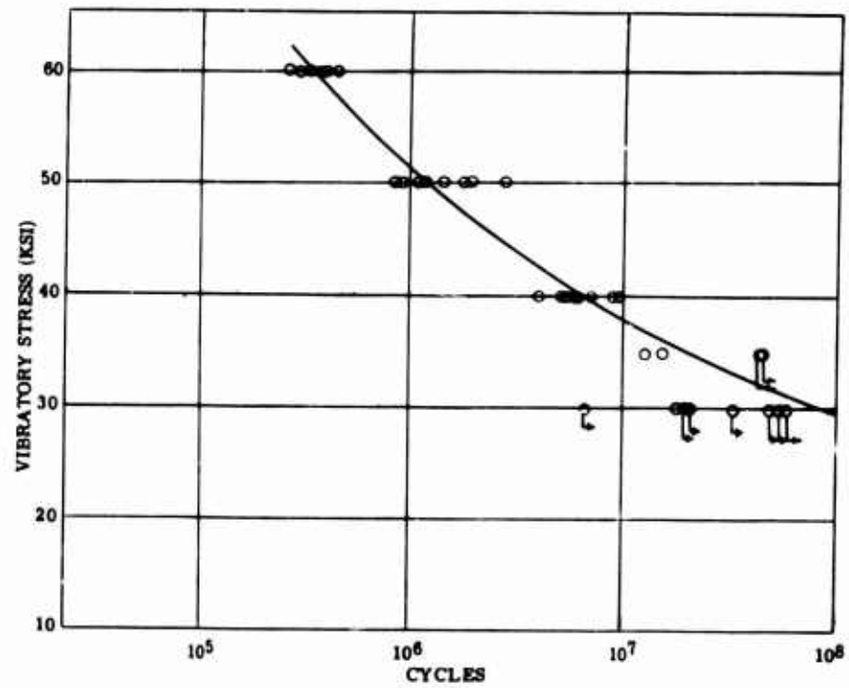

Figure 5. Ti-6Al-6V-2Sn Axial Tension-Tension Fatigue Results, Mean Stress = 70,000 psi.

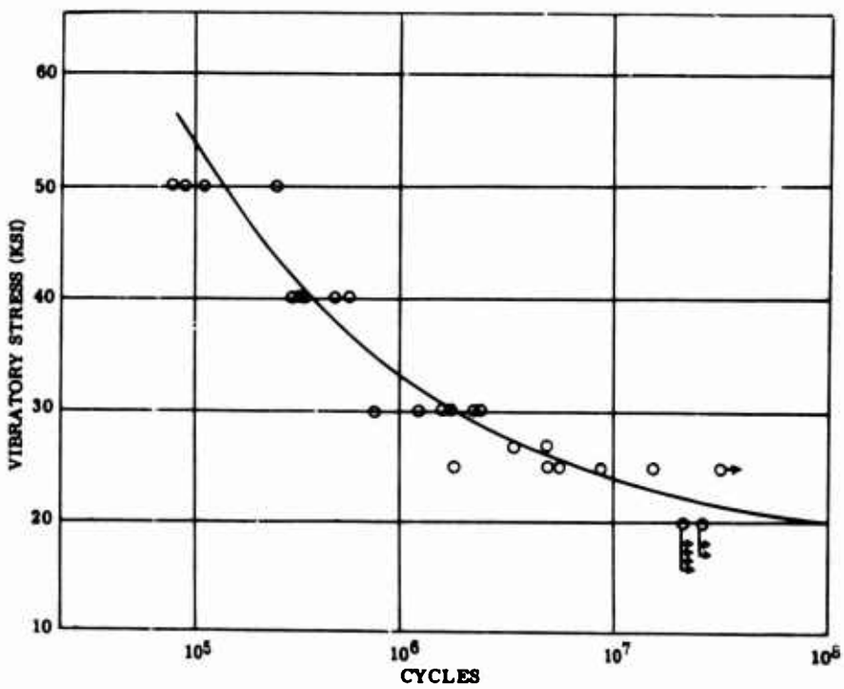

Figure 6. Ti-13V-11Cr-3Al Axial Tension-Tension Fatigue Results, Mean Stress = 70,000 psi.

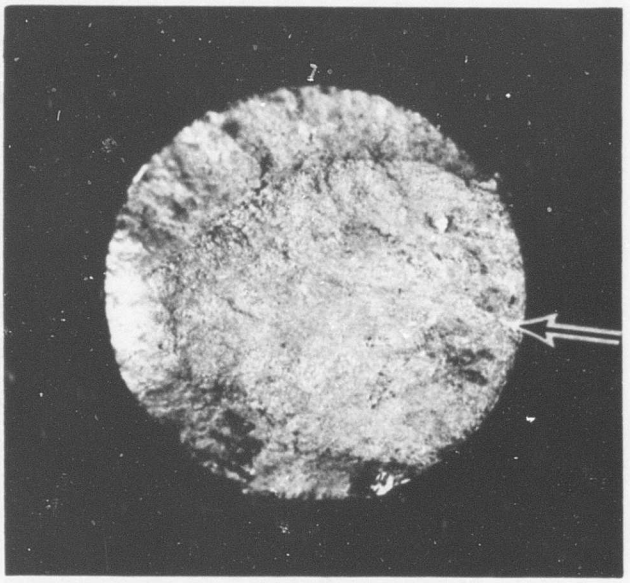

Figure 7. Fatigue Fracture Surface of Ti-6Al-6V-2Sn Axial Tension-Tension Fatigue Specimen.

Note: Arrows on both photographs indicate origin of failure.

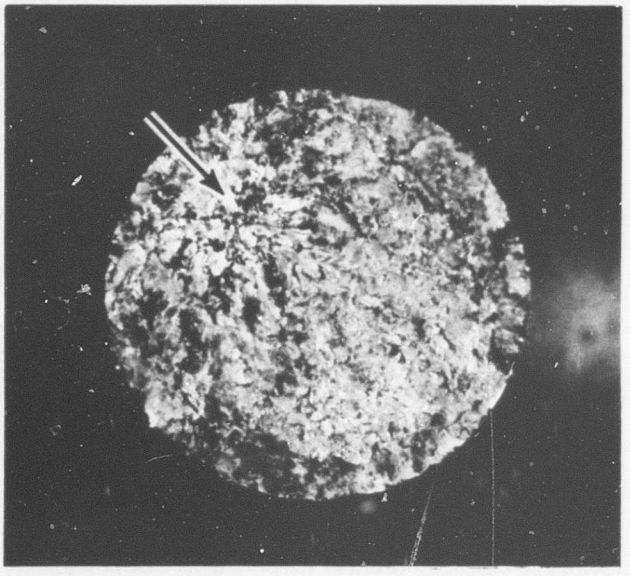

Figure 8. Fatigue Fracture Surface of Ti-13V-11Cr-3Al Axial Tension-Tension Fatigue Specimen.

SECTION II - JOINT FATIGUE TESTS

EXPERIMENTAL PROCEDURE

Ten forgings of each alloy were cut into specimen blanks, twelve blanks per forging, and were identified as shown in Figure 10. The blanks were machined to the required specimen dimensions shown in Figure 11.

Randomization of test specimens was done in the same manner described in the section on axial tension-tension specimens. Initial randomization was made based on specimen identification; groups of specimens were assigned to specific surface conditions and loads from this list; the list was randomized a second time to avoid effects due to calendar time or the fatigue machine.

Constant-load fatigue machines, Sonntag Scientific Corporation Model SF-1-U, with five-to-one amplifiers were used to test the joint fatigue specimens. These fatigue machines were shown in Figure 3. An Ellis Company Model BA-12 bridge amplifier and cathode ray oscilloscope were used to measure the applied fatigue loads.

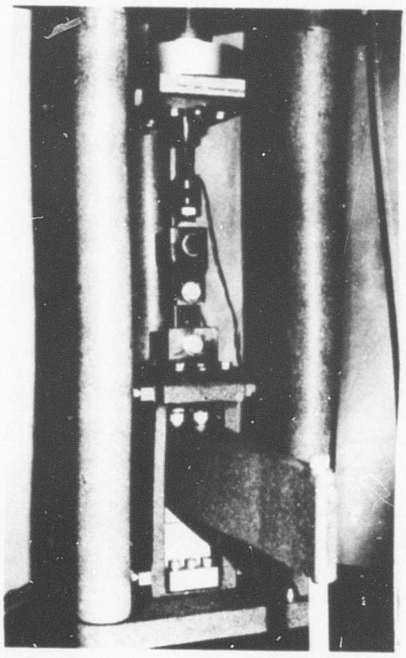

Figure 9. Joint Specimen Installed in Five-to-One Amplifier on SF-1-U.

Figure 9 shows a specimen installed in series with a load cell in a five-to-one amplifying system on a fatigue machine. The calibrated load cell was used to measure the static and dynamic loads applied to each specimen.

The procedure used to analyze the fatigue data was the same as that used for the axial tension-tension specimens.

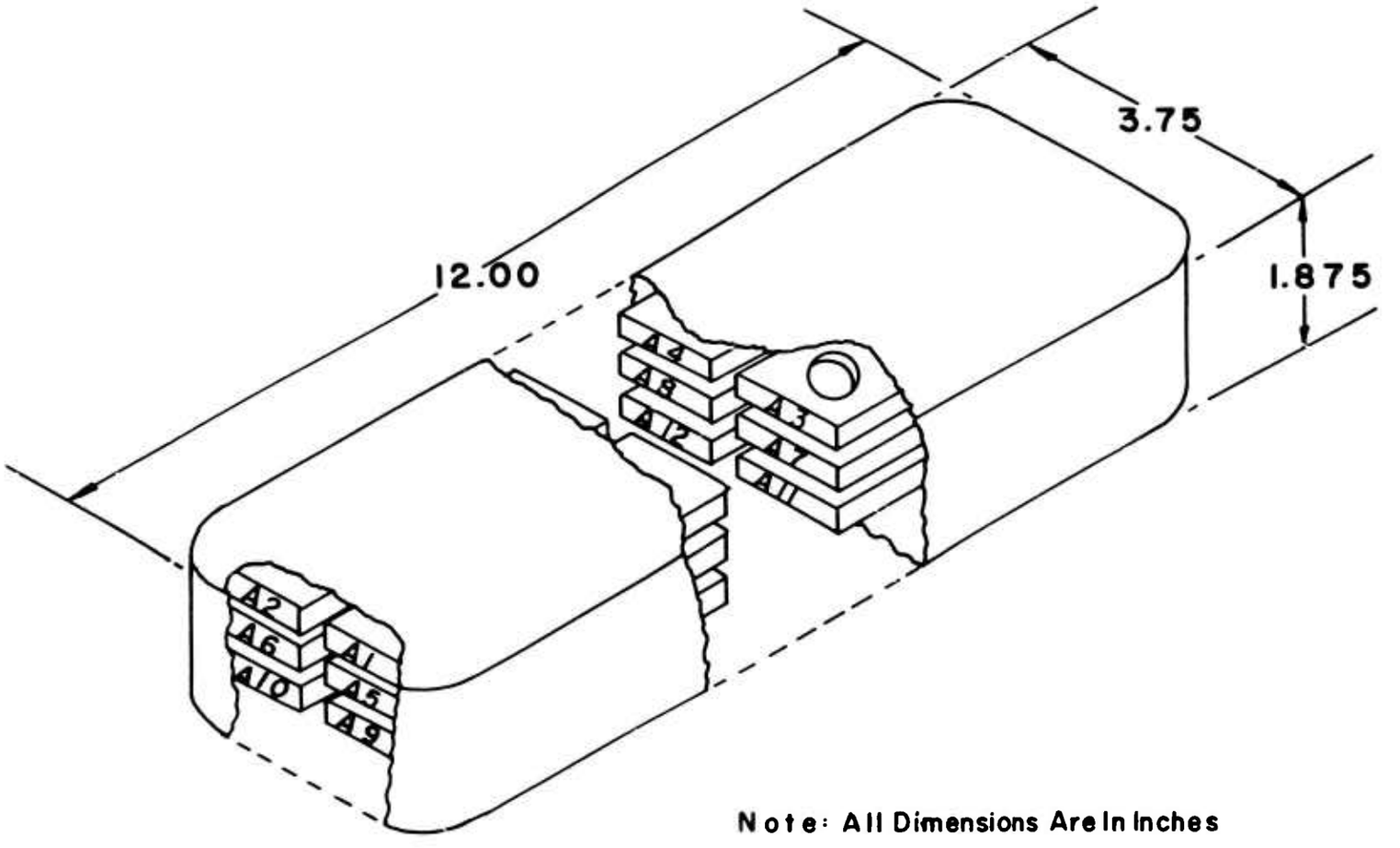

Figure 10 Location of Joint Fatigue Specimens in Forging.

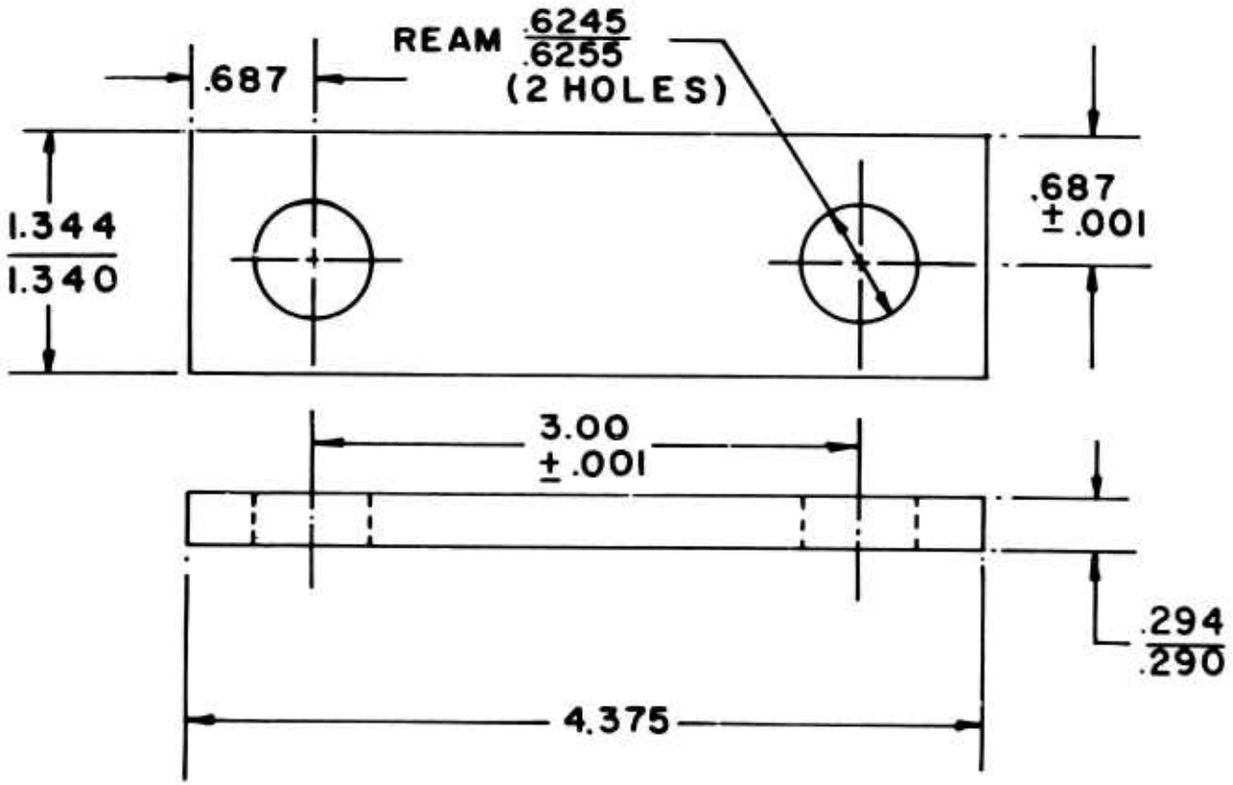

Note: All Dimensions Are In Inches.

Figure 11. Dimensioned Sketch of Joint Fatigue Specimen .

The specimens were tested with holes in three conditions: reamed, shot peened, and expanded. All holes were drilled and reamed in a fixture in accordance with normal shop practice. Shot peened specimens were prepared using S-110 shot to a 6A intensity. For the expanded specimens, expansion of 0.0005 inch on the diameter was accomplished using a roller burnishing tool in the bore at one end of the joint specimen and a bearingizing tool in the bore at the opposite end of the joint specimen. For all three hole conditions tested, the clearance between the bolt and hole was approximately 0.001 inch.

The roller burnishing tool uses smooth tapered pins rotating on a smooth tapered mandrel, as illustrated in Figure 12. The amount of expansion is controlled by mechanical stops which limit the travel of the mandrel, forcing the pins into the surface of the hole. The bearingizing tool imparts a burnishing and peening effect with smooth straight pins rotating on a straight mandrel with ground flats on its circumference. The amount of expansion is controlled by the dimensions of the bearingizing tool. The straight pins are forced into the surface of the hole by a cam action; i.e., the pins are driven from the minimum diameter at the center of the ground flats to the maximum diameter at the edges formed between the ground flats.

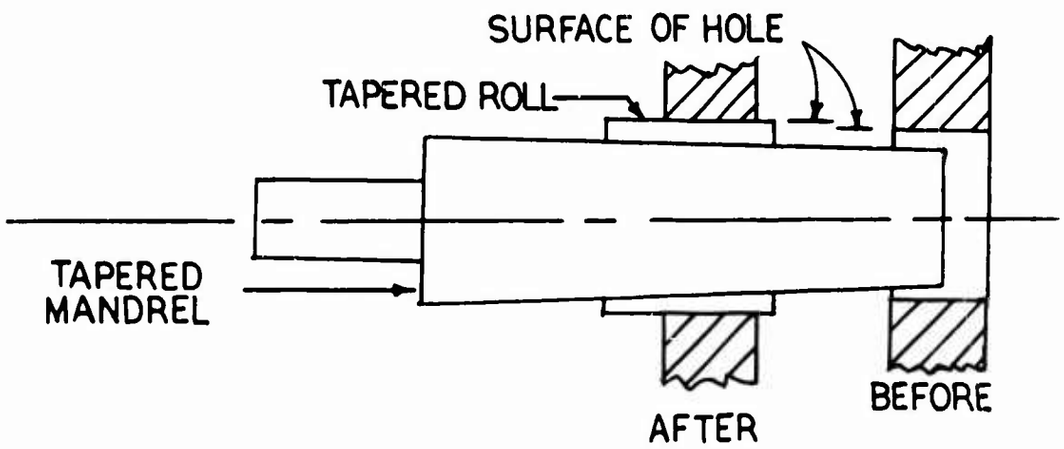

Figure 12. Schematic of Roller Burnishing Tool.

EXPERIMENTAL RESULTS AND DISCUSSION OF RESULTS

A minimum of 30 specimens of both alloys were tested at a nominal steady stress (not allowing for the stress concentration factor of the hole) of 21,600 psi. This configuration of joint fatigue specimen has a theoretical stress concentration factor, due to the hole and geometry, of 2.7, based on the theory described in Reference 5. The fatigue test results are illustrated in the form of S/N curves, shown in Figures 13 through 18. Figures 15 and 18 show the specimen failures originating at the holes processed with the roller burnishing tool (indicated by the symbol ▽) and the failures originating at the holes processed with the bearingizing tool (indicated by the symbol ◥). The results of the fatigue data shown in Figures 13 through 18 are summarized in Table II. The mean endurance strength is given without allowing for the stress concentration factor of the hole.

TABLE II

JOINT FATIGUE TEST RESULTS

Alloy and Condition	E_T (psi)	α	γ	s (psi)*	$\bar{X}$ (psi)*	$s/\bar{X}$ (%)*
Ti-6Al-6V-2Sn						
Reamed	4,850	2,400	.667	853	4,970	17.2
Shot Peened**	-	-	-	-	-	-
Expanded	10,300	1,440	.667	1,350	10,300	13.1
Ti-13V-11Cr-3Al						
Reamed	4,340	1,440	.667	1,040	4,410	23.6
Shot Peened	7,080	1,440	.667	1,250	7,160	17.5
Expanded	8,510	1,440	.667	847	8,570	9.9

*Applicable at 10^8 cycles of vibratory stress.

**Because of the large scatter in the data for the Ti-6Al-6V-2Sn shot peened joint specimens, the mean S/N curve, shown as a dotted line in Figure 14, was only estimated. Therefore, the curve shape parameters, mean endurance strength, standard deviation, and coefficient of variation are not presented.

Figures 19 and 20 illustrate the mean curves (without points) for each condition of each alloy. For each condition, Ti-6Al-6V-2Sn is superior to Ti-13V-11Cr-3Al. Surface working of the holes (shot peening or expanding) improves the endurance strength of the joint, with expanding giving the greater improvement.

Table II illustrates the superiority of expanding over shot peening of relatively small holes by giving a higher endurance strength and a smaller standard deviation. Expanding is considered to be a more economical process than shot peening for preparing close-tolerance, cold-worked holes. Normally, for a shot peened hole, the hole is drilled and reamed in a fixture, removed for shot peening, and set up once again for a final reaming or honing operation. However, the three operations are combined into one for the expanding process.

The roller burnishing tool is the preferred expanding tool over the bearingizing tool. Greater flexibility of this tool is possible relative to hole tolerances and amounts of expansion. No significant difference in fatigue strength was apparent as a function of the expanding tool, within the limit of the same amount of expansion, 0.0005 inch, for both tools applied in this test series.

Figures 21 and 22 are typical joint fatigue fracture surfaces of both alloys for each condition.

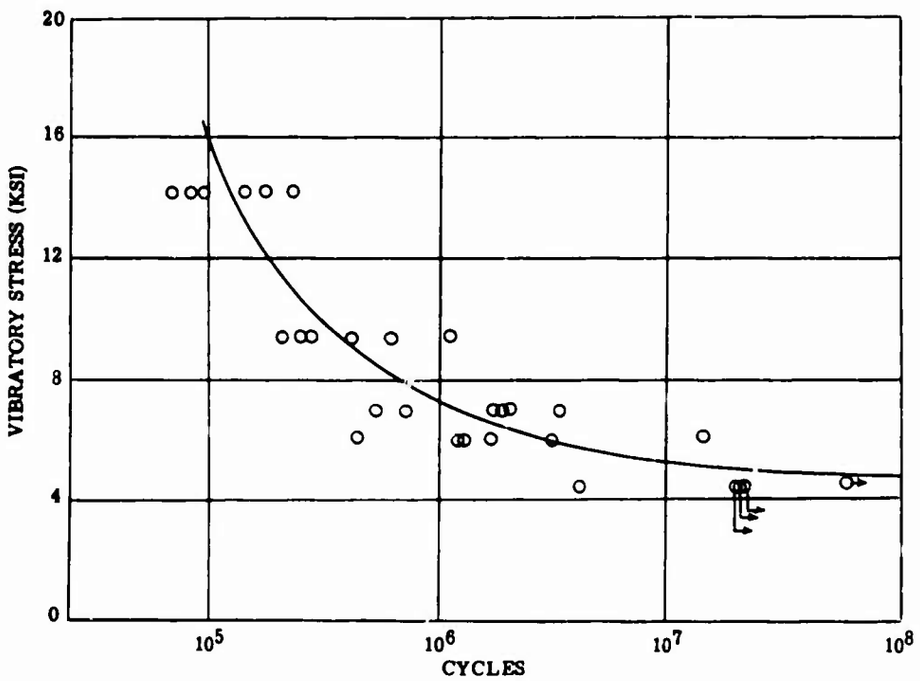

Figure 13. Fatigue Test Results, Ti-6Al-6V-2Sn Joint Specimens, Reamed Condition, Mean Stress = 21,600 psi.

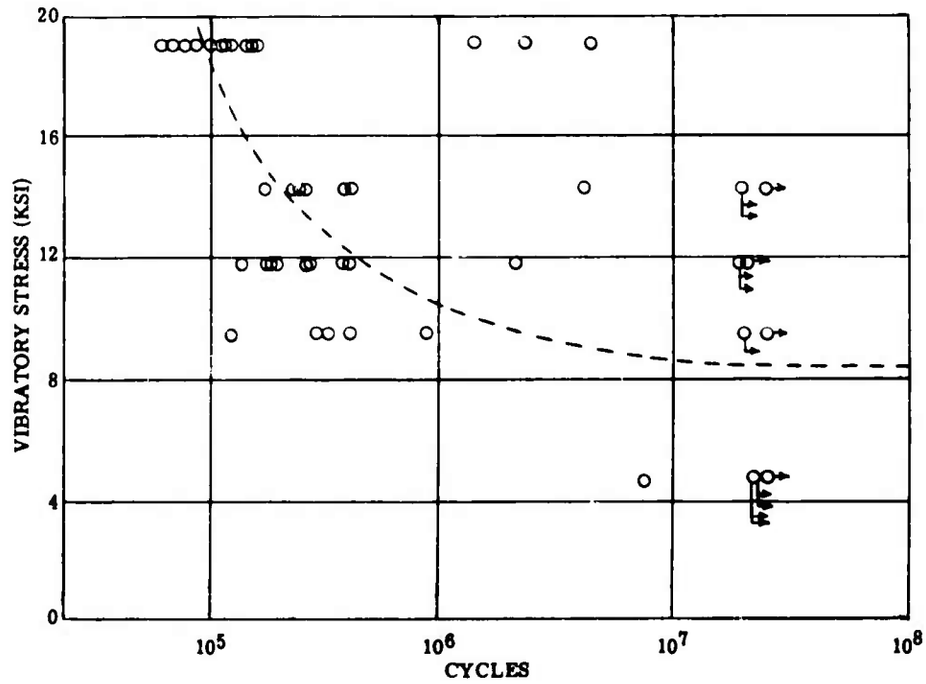

Figure 14. Fatigue Test Results, Ti-6Al-6V-2Sn Joint Specimens, Shot Peened Condition, Mean Stress = 21,600 psi.

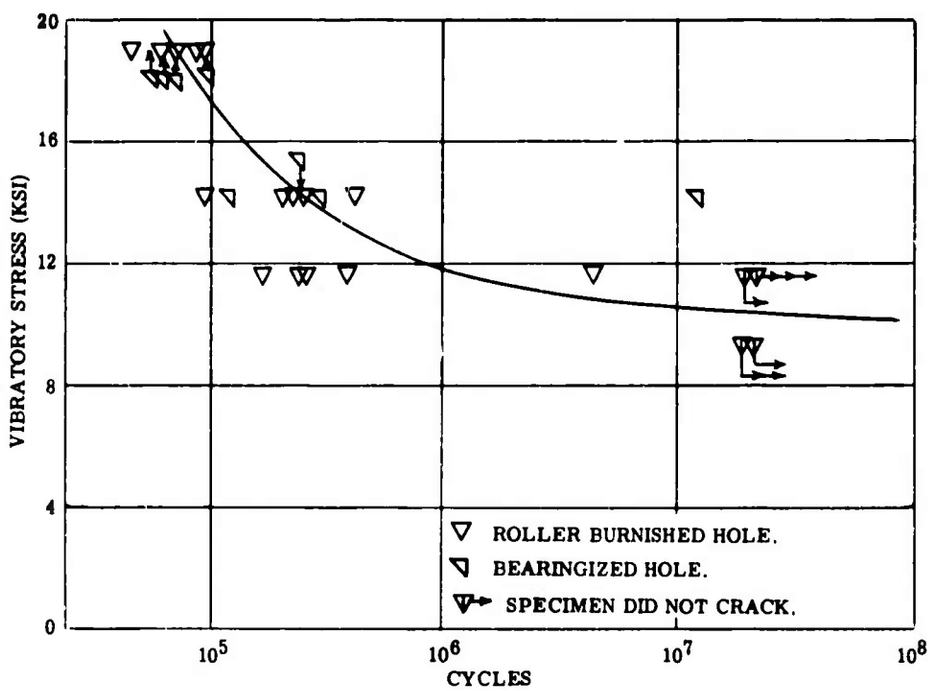

Figure 15. Fatigue Test Results, Ti-6Al-6V-2Sn Joint Specimens, Expanded Condition, Mean Stress = 21,600 psi.

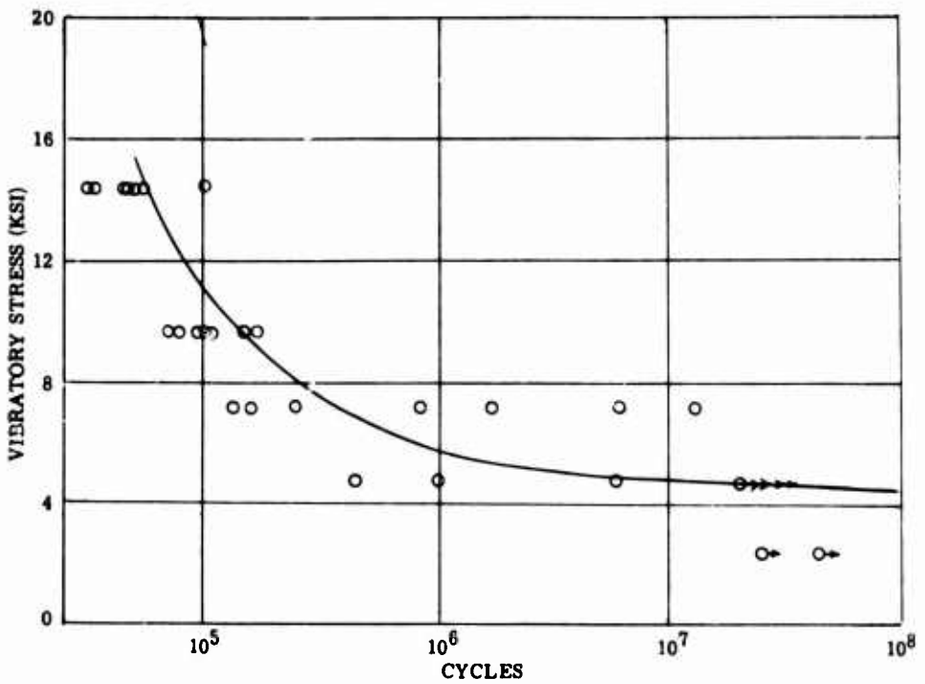

Figure 16. Fatigue Test Results, Ti-13V-11Cr-3Al Joint Specimens, Reamed Condition, Mean Stress = 21,600 psi.

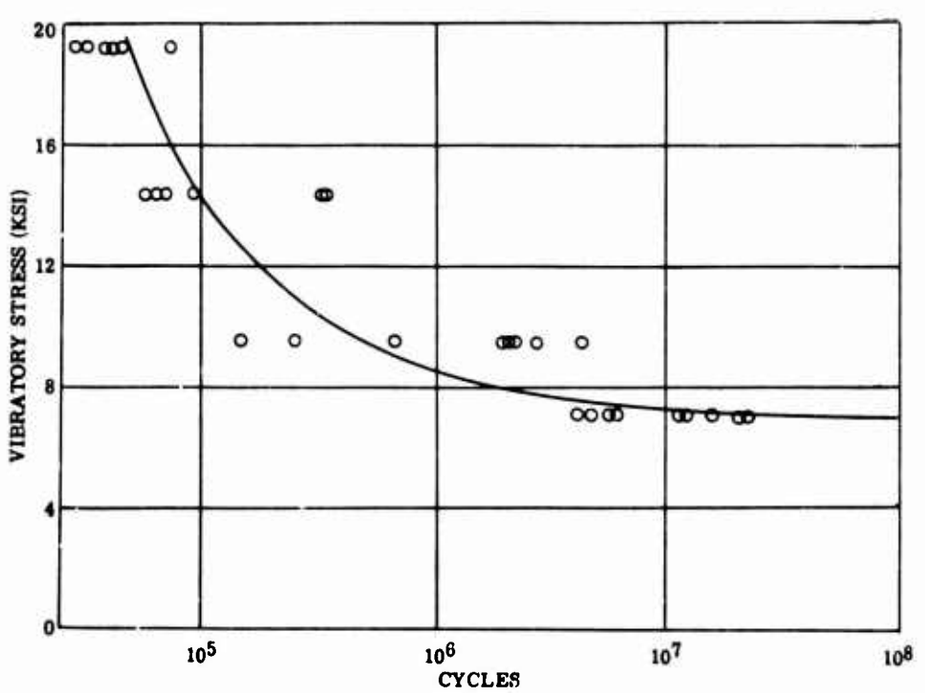

Figure 17. Fatigue Test Results, Ti-13V-11Cr-3Al Joint Specimens, Shot Peened Condition, Mean Stress = 21,600 psi.

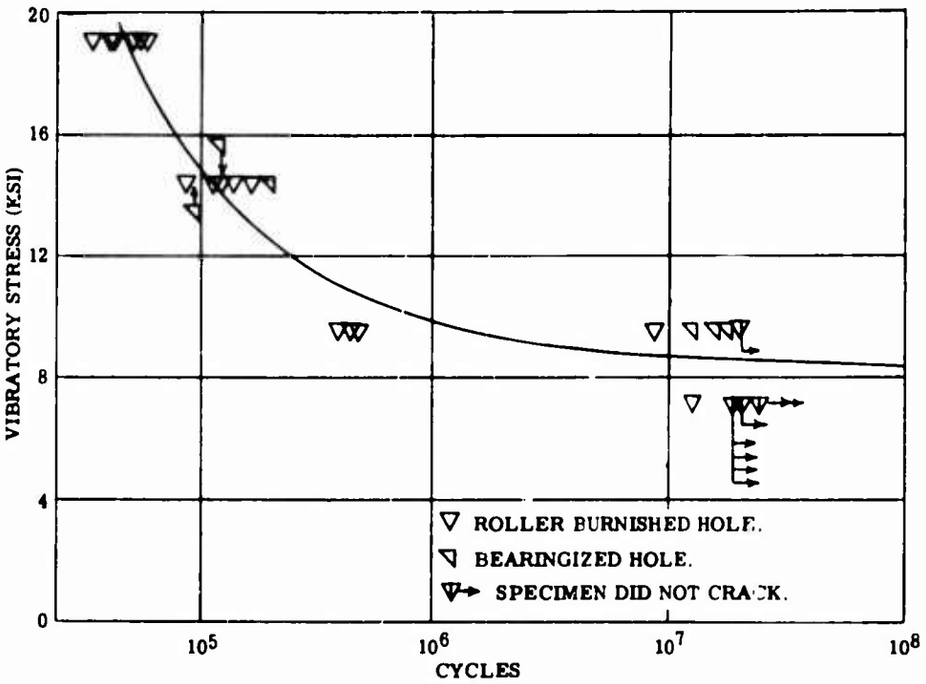

Figure 18. Fatigue Test Results, Ti-13V-11Cr-3Al Joint Specimens, Expanded Condition, Mean Stress = 21,600 psi.

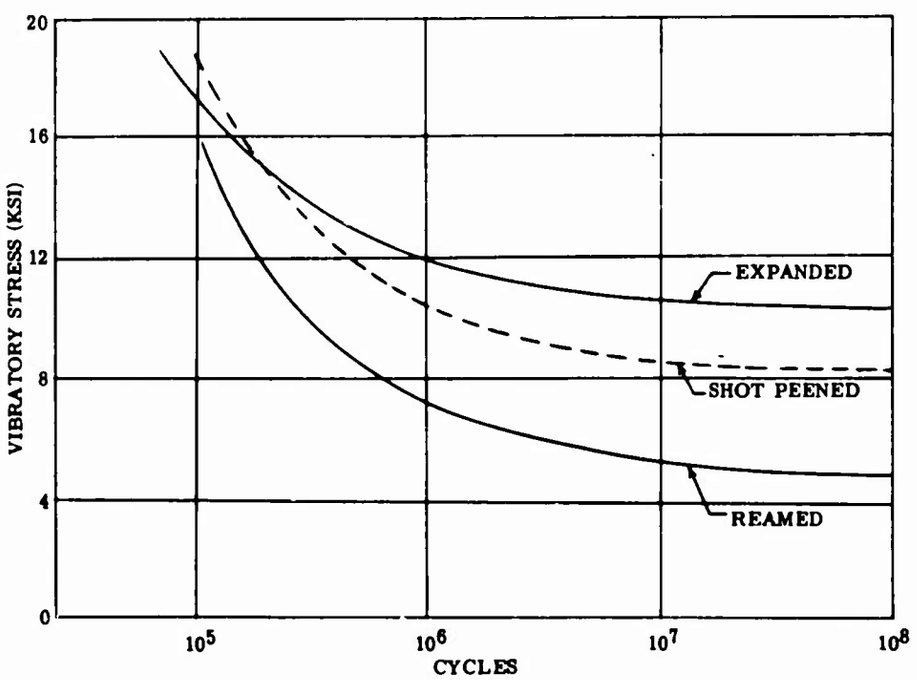

Figure 19. Mean Curves of Ti-6Al-6V-2Sn Joint Specimens for Three Hole Conditions, Mean Stress = 21,600 psi.

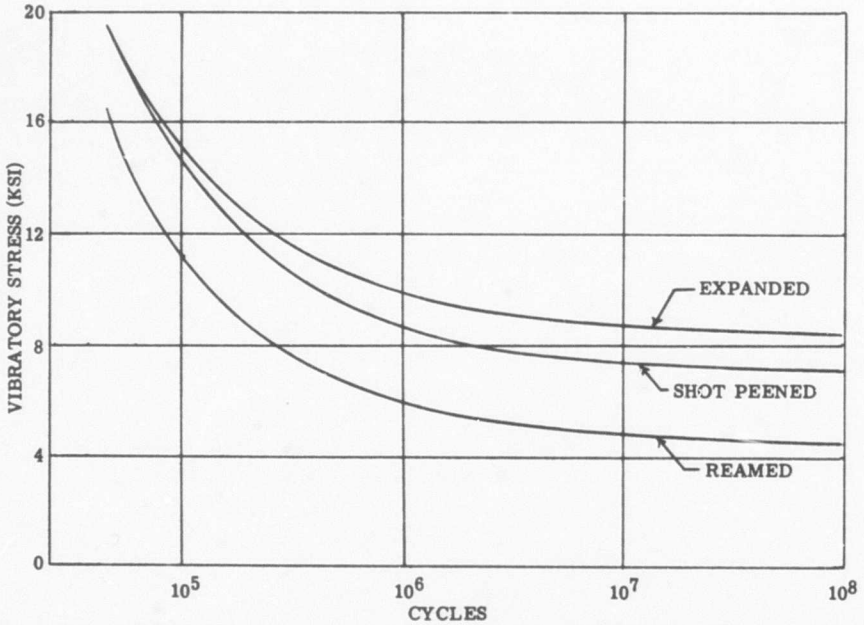

Figure 20. Mean Curves of Ti-13V-11Cr-3Al Joint Specimens for Three Hole Conditions, Mean Stress = 21,600 psi.

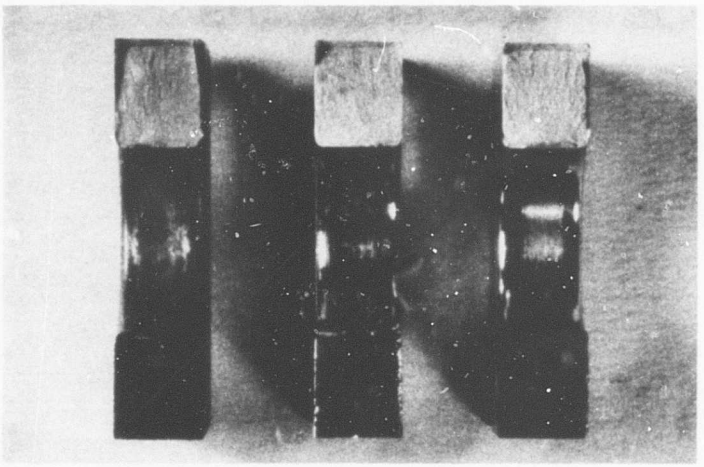

Figure 21. Typical Joint Fatigue Fracture Surfaces, Ti-6Al-6V-2Sn.

Note: Fractures, from left to right, are shot peened, reamed, and expanded.

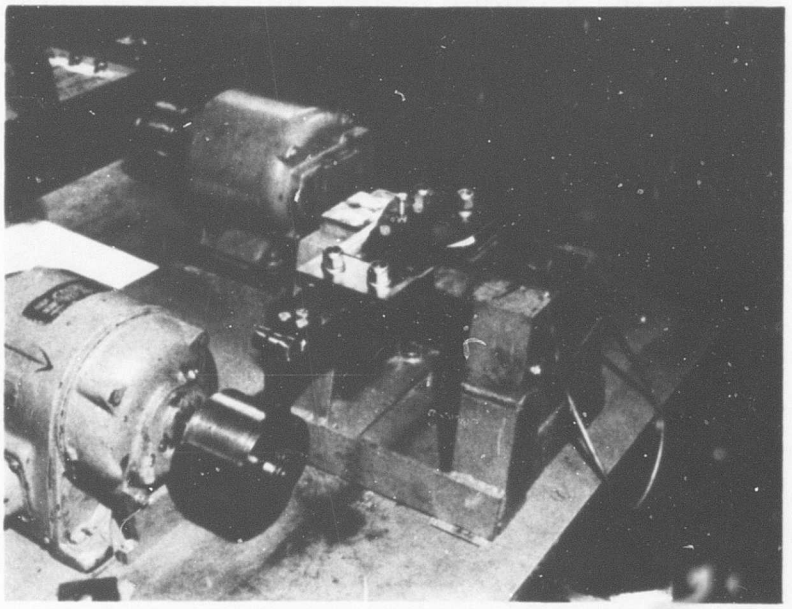

Figure 22. Typical Joint Fatigue Fracture Surfaces, Ti-13V-11Cr-3Al.

Note: Fractures, from left to right, are shot peened, reamed, and expanded.

SECTION III - FATIGUE CRACK PROPAGATION TESTS

EXPERIMENTAL PROCEDURE

Twelve specimens of each alloy were tested, four specimens at each of three test levels:

1. + 13,400 ± 5,000 psi
2. + 13,400 ± 10,000 psi
3. + 20,000 ± 5,000 psi

Each specimen was machined from a forging, Figure 23, to dimensions shown in Figure 24. After machining, the specimens were shot peened with S-110 shot to a 6A intensity. Randomization of forgings was accomplished relative to test level and type of test in the same manner described previously.

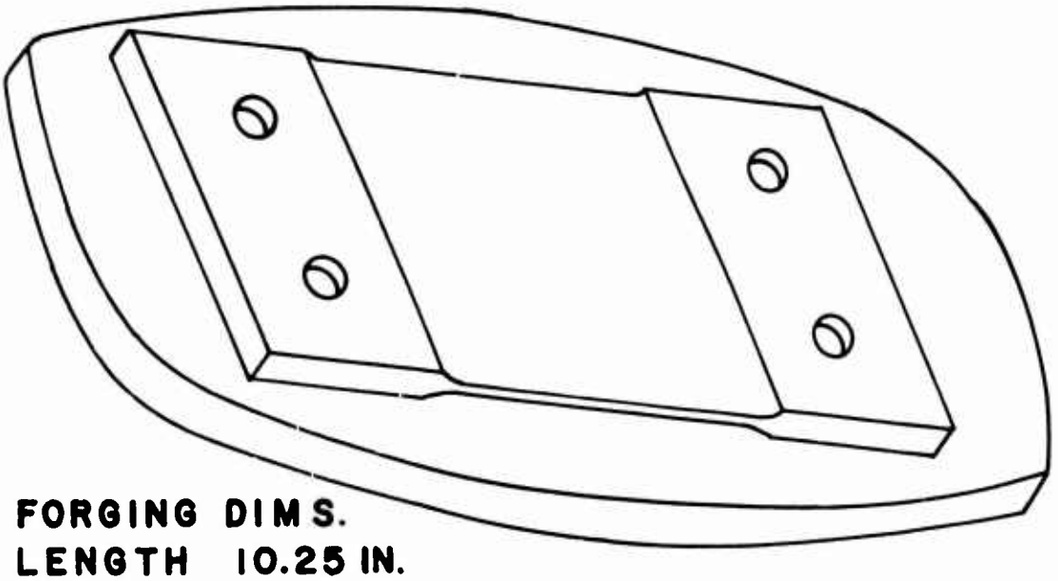

Figure 23. Location of Crack Propagation Specimen in Forging.

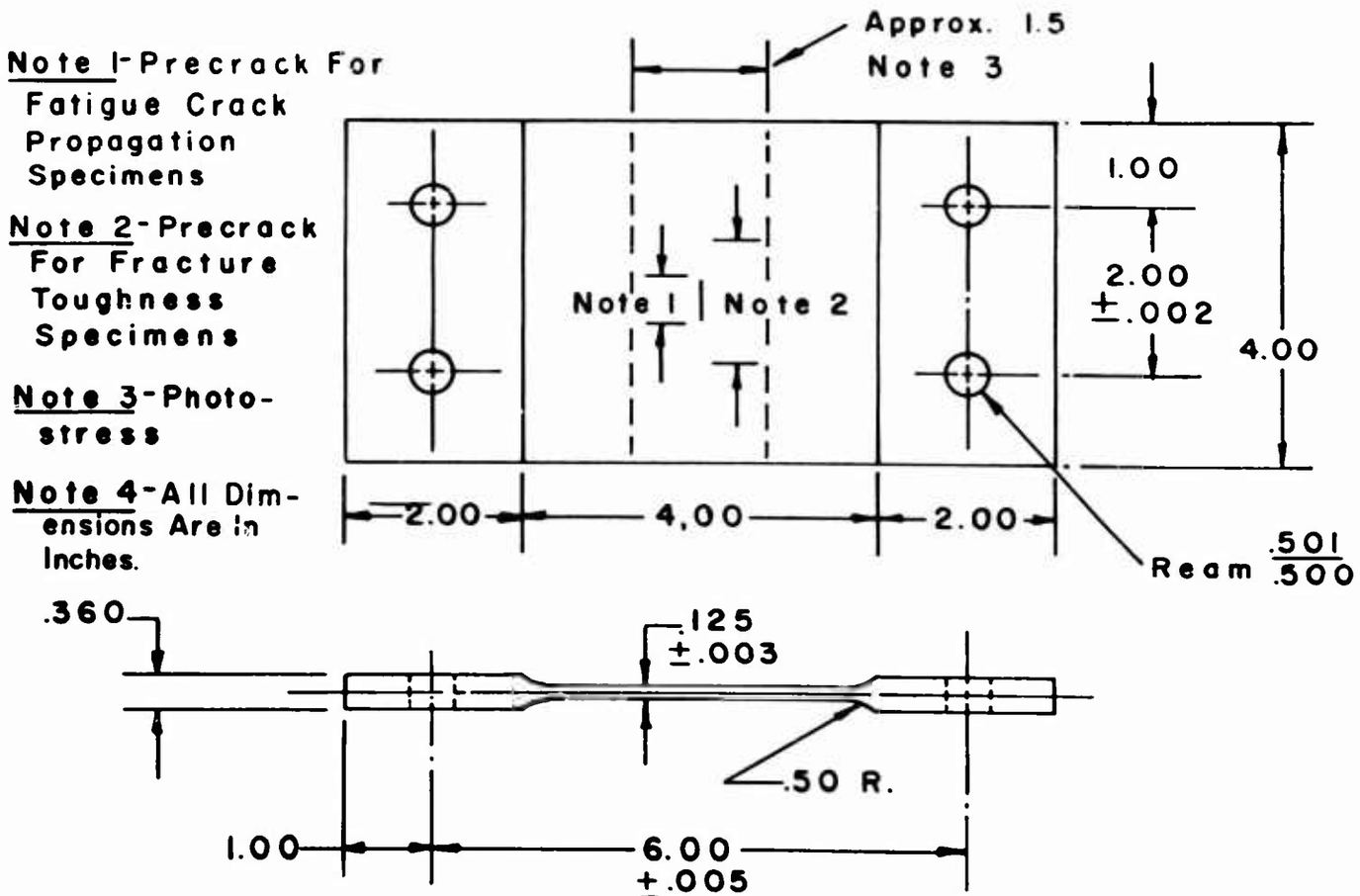

Figure 24. Crack Propagation Specimen.

The specimens were precracked by flexing between a pair of preloaded 1/8-inch-wide knife edges with an electric-motor-driven Krouse eccentric head, Figure 25. The length of the precrack was controlled to approximately 3/8 inch by a microwire technique (cementing small copper wires, which are connected to a relay in the motor control circuit to the specimen at the desired end points of the crack).

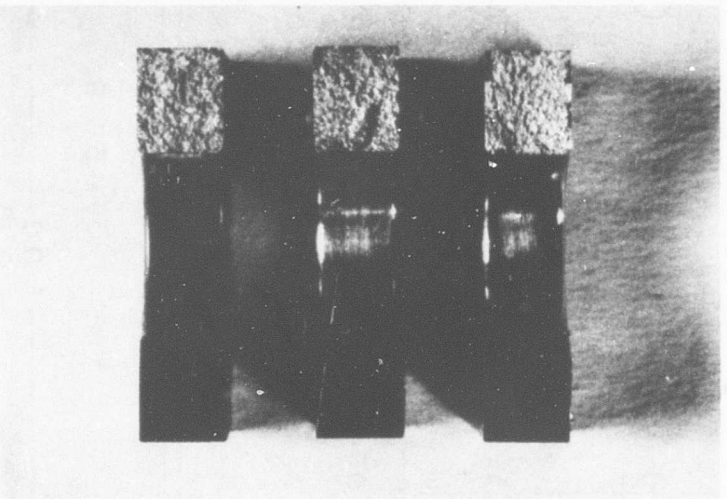

Figure 25. Crack Propagation Precrack Setup.

Fatigue crack propagation tests were conducted on a Wiedemann - Baldwin IV-4 constant-load fatigue machine with a five-to-one load amplifier. The overall test setup is shown in Figure 26.

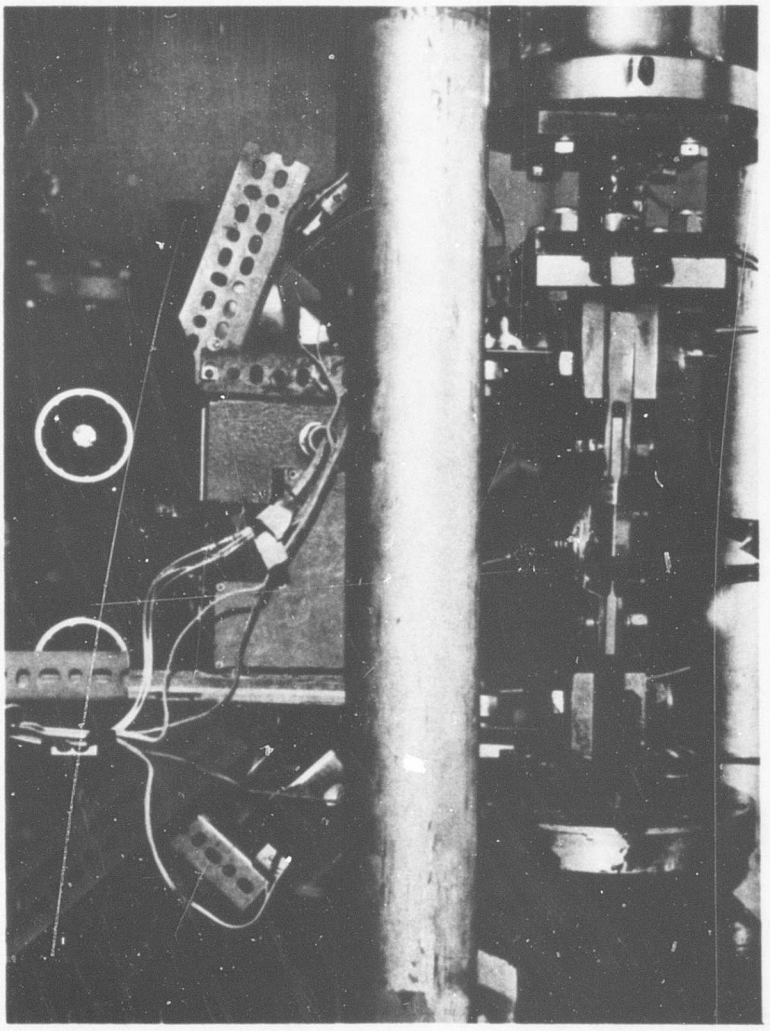

Figure 26. Fatigue Crack Propagation Test Setup on the IV-4.

A calibrated load cell in series with the specimen was used to control the applied loads. Prior to testing, a strip of birefringent plastic, 1-1/2 by 4 inches, was bonded to the specimen in the pre-crack area. A close-up of a specimen mounted in the fatigue machine is shown in Figure 27.

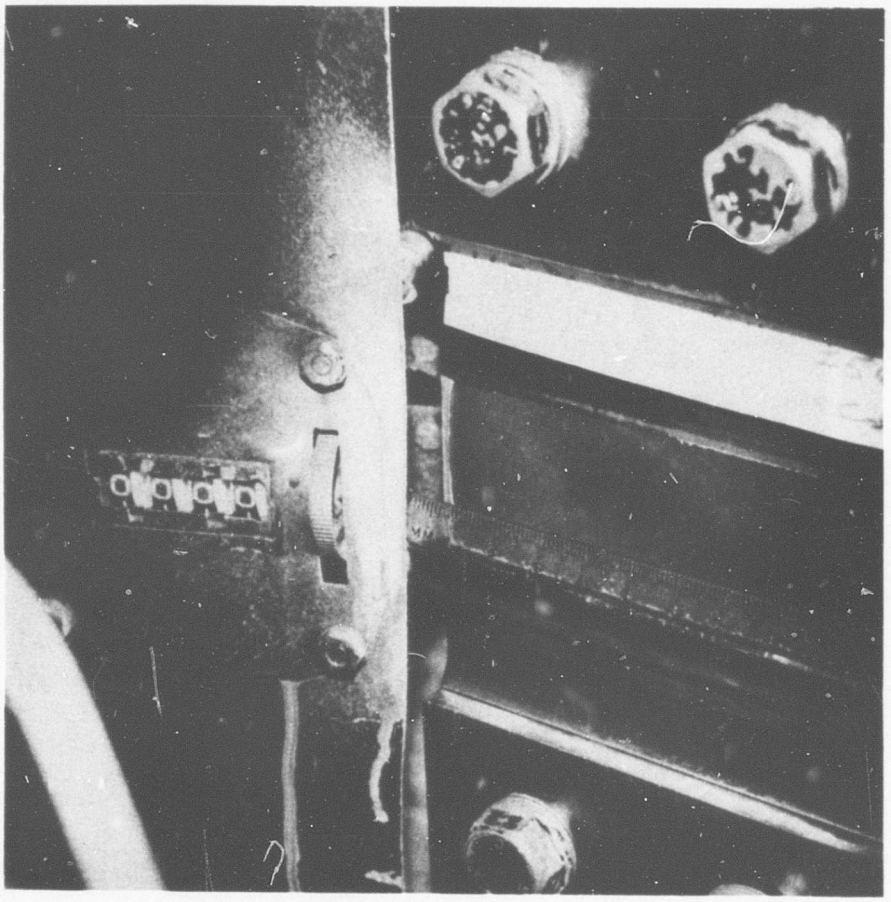

Figure 27. Fatigue Crack Propagation Specimen Mounted in the IV-4.

The crack length was measured after testing by projecting photographs of the specimen taken with polarized light at the maximum load applied by the fatigue machine. A scale, attached to the specimen, served as a base for the measurements taken. Four IBM 7094 digital computer routines were used to calculate and compare the following:

1. Stress intensity factor, K, psi $\sqrt{\text{inch}}$, where K is calculated from the equation

$$K = \frac{S_g \sqrt{a} \sqrt{4 + 2\,(a/b)^4}}{2 - (a/b)^2 - (a/b)^4}$$

2. Crack propagation rate, microinches per cycle.

3. Plots of fatigue crack length versus number of cycles of vibratory load.

4. Plots of stress intensity factor versus fatigue crack propagation rate. A least-squares-fit curve was obtained for the slow and fast propagation portions of these curves by means of another computer routine.*

EXPERIMENTAL RESULTS AND DISCUSSION OF RESULTS

The computer-reduced data are given in the following two graphical forms:

1. Crack length versus cycles of vibratory load, Figures 28 through 33.

2. Stress intensity factor versus fatigue crack propagation rate, Figures 34 and 35.

For comparison of the two alloys at each stress level, the fatigue crack propagation stress intensity factor at static failure and the cycles to failure from a 3/4-inch initial crack length are both given in Table III. The arithmetic average of the cycles to failure and the stress intensity factor at static failure for four test specimens are listed. An initial crack length of 3/4 inch was chosen to eliminate variations in the effective specimen width due to the initial crack orientation and length produced by the precrack techniques.

The slow crack propagation portions of the stress intensity factor versus crack propagation rate plots are defined only by a horizontal dotted line for the Ti-13V-11Cr-3Al alloy. Not enough data points were available in the slow crack propagation region to determine the slope of this line accurately. This lack of data is due to the relatively small amount of slow crack propagation before the onset of rapid fatigue crack propagation in this alloy.

*A more complete description of the computer routines for reduction of these data is given in Reference 2.

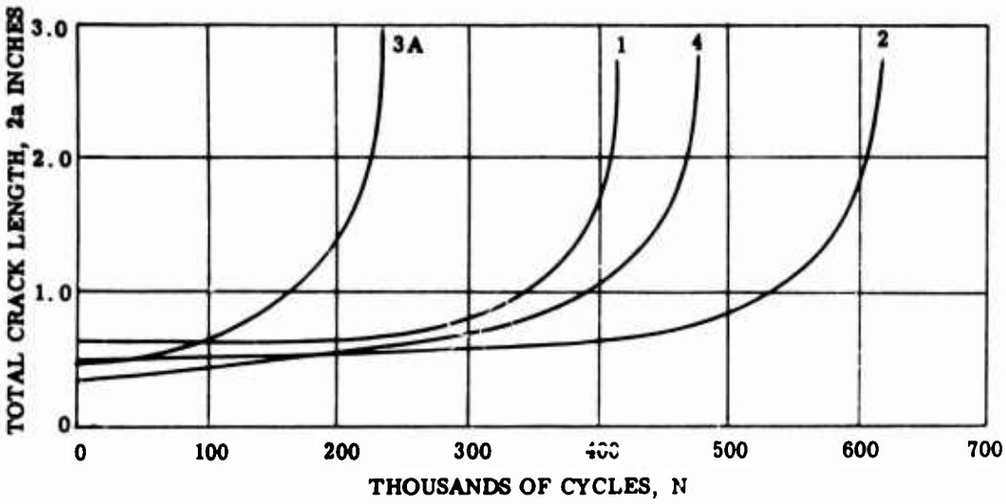

Figure 28. Crack Length versus Cycles to Failure for Ti-6Al-6V-2Sn, First Stress Level = 13,400 ± 5,000 psi, Specimens 1, 2, 3A, and 4.

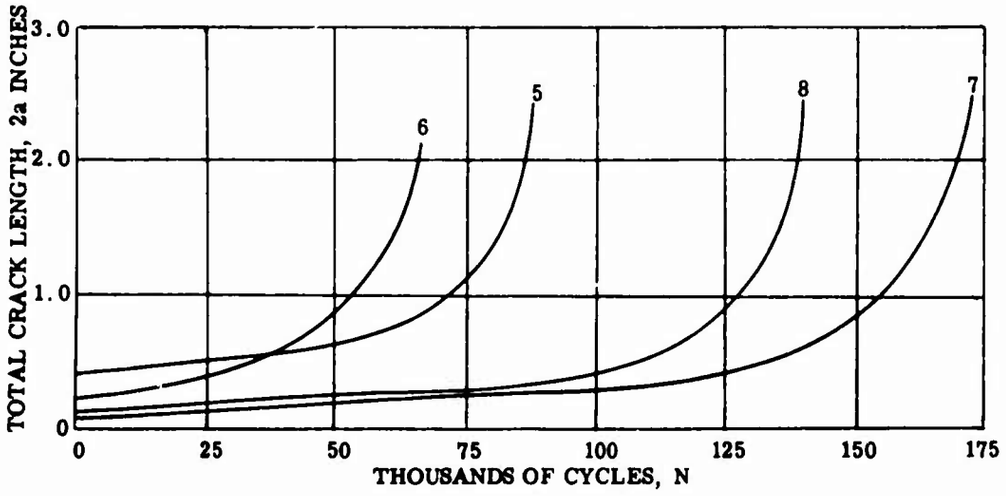

Figure 29. Crack Length versus Cycles to Failure for Ti-6Al-6V-2Sn, Second Stress Level = 13,400 ± 10,000 psi, Specimens 5, 6, 7, and 8.

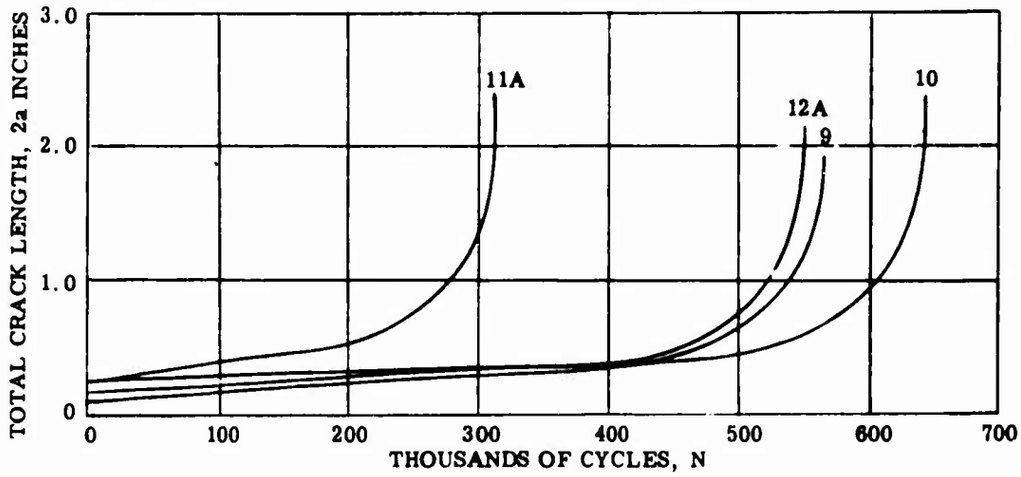

Figure 30. Crack Length versus Cycles to Failure for Ti-6Al-6V-2Sn, Third Stress Level = 20,000 ± 5,000 psi, Specimens 9, 10, 11A,and 12A.

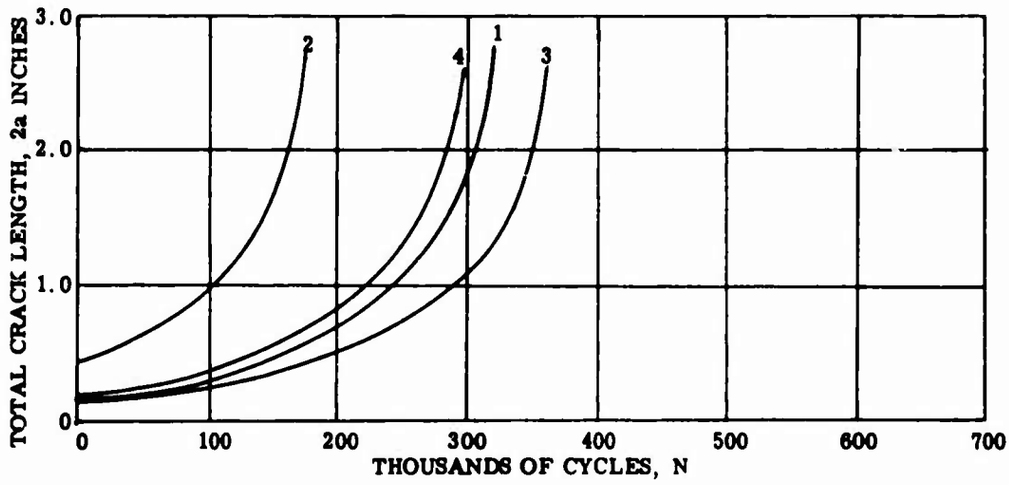

Figure 31. Crack Length versus Cycles to Failure for Ti-13V-11Cr-3Al, First Stress Level = 13,400 ± 5,000 psi, Specimens 1, 2, 3, and 4.

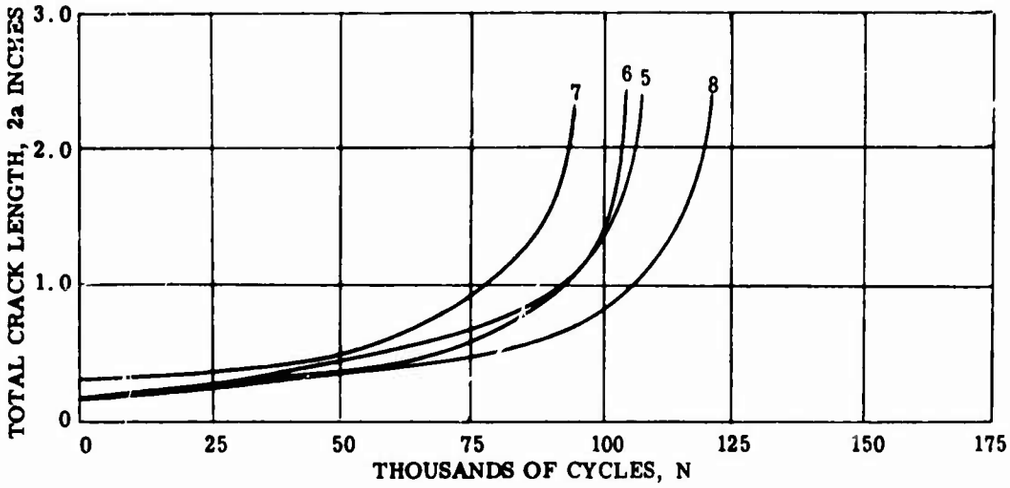

Figure 32. Crack Length versus Cycles to Failure for Ti-13V-11Cr-3Al, Second Stress Level = 13,400 ± 10,000 psi, Specimens 5, 6, 7, and 8.

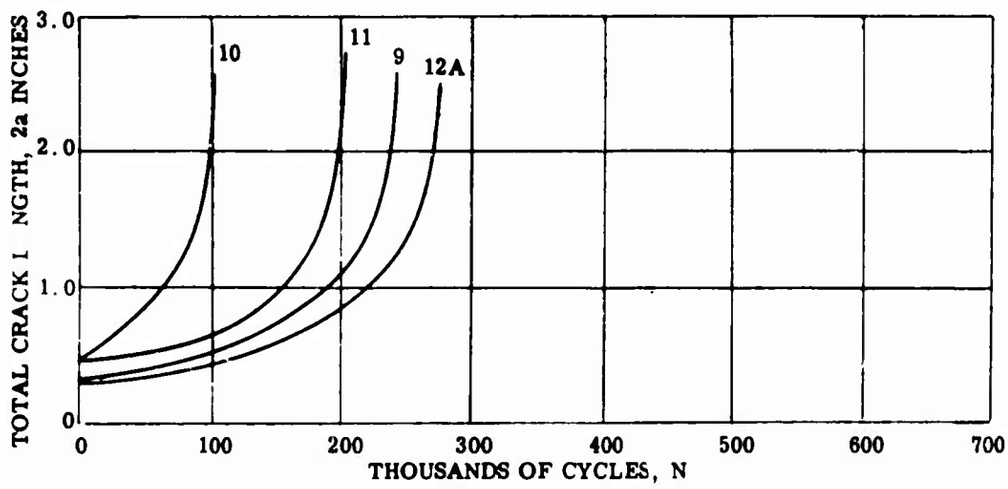

Figure 33. Crack Length versus Cycles to Failure for Ti-13V-11Cr-3Al, Third Stress Level = 20,000 ± 5,000 psi, Specimens 9, 10, 11, and 12A.

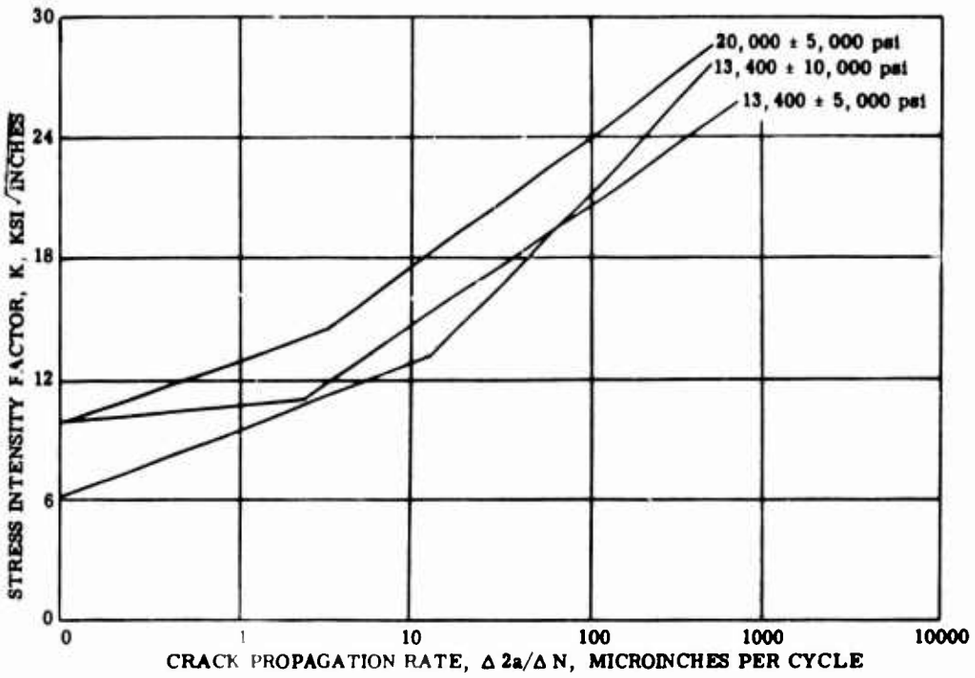

Figure 34. Mean Curve of Stress Intensity Factor versus Crack Propagation Rate for Ti-6Al-6V-2Sn at Three Stress Levels.

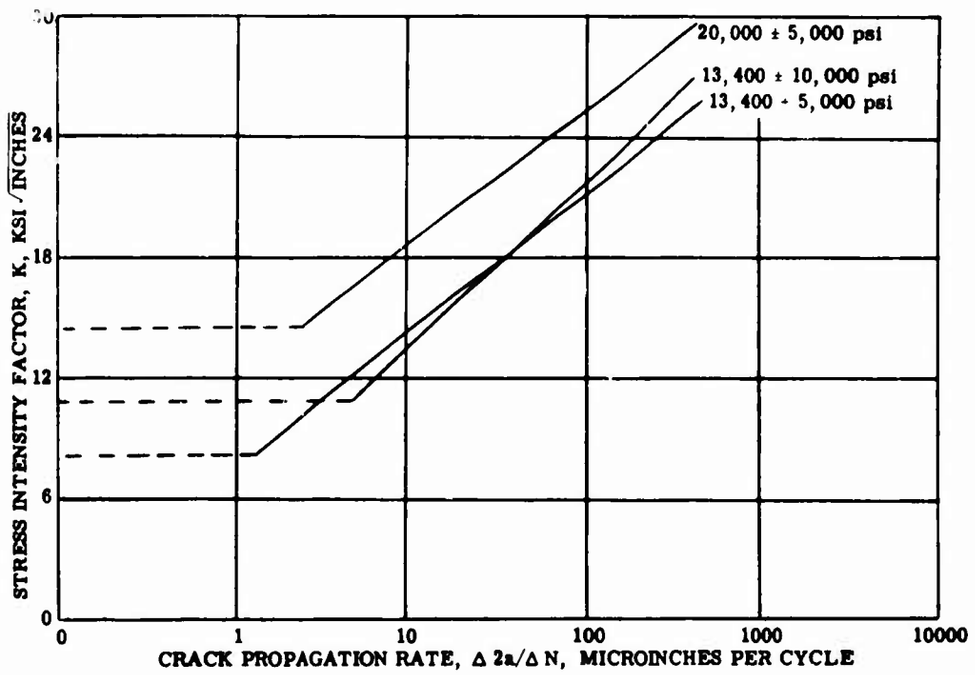

Figure 35. Mean Curve of Stress Intensity Factor versus Crack Propagation Rate for Ti-13V-11Cr-3Al at Three Stress Levels.

TABLE III

FATIGUE CRACK PROPAGATION TEST RESULTS

Item	Cycles to Failure	K (at static fracture) (psi $\sqrt{\text{inch}}$)
Ti-6Al-6V-2Sn		
+ 13,400 ± 5,000 psi	130,000	24,200
+ 13,400 ± 10,000 psi	25,000	27,900
+ 20,000 ± 5,000 psi	55,000	28,400
Ti-13V-11Cr-3Al		
+ 13,400 ± 5,000 psi	112,000	23,500
+ 13,400 ± 10,000 psi	29,000	26,700
+ 20,000 ± 5,000 psi	80,000	31,100

Examination of the specimen fracture surfaces revealed a relatively rougher fracture surface for the Ti-13V-11Cr-3Al alloy than for the Ti-6Al-6V-2Sn alloy (Figure 36). This condition was attributed to the larger grain size of the Ti-13V-11Cr-3Al alloy.

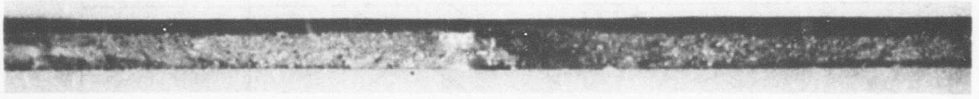

Ti-6Al-6V-2Sn

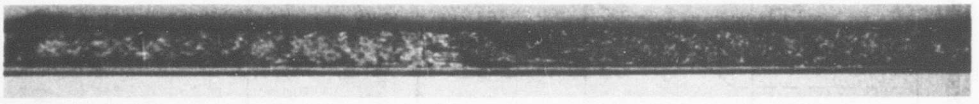

Ti-13V-11Cr-3Al

Figure 36. Typical Fracture Surfaces for Fatigue Crack Propagation Specimens.

SECTION IV - FRACTURE TOUGHNESS TESTS

EXPERIMENTAL PROCEDURE

Fracture toughness specimens were precracked in the same manner as the fatigue crack propagation specimens. The precrack was then extended to approximately 1 inch (Figure 24) by running at a low vibratory stress in a fatigue machine. The same microwire technique described previously was used to control the length of the crack.

Fracture toughness testing was done in a Riehle PS-60 tensile testing machine. The overall test setup is shown in Figure 37. Test equipment and procedures followed the recommendations of Fracture Toughness Testing in Reference 4. A compliance gage, patterned after the unit described in Reference 1, was used to measure crack extension. A strain-gaged bent beam was used to measure compliance gage vertical displacement so that the electrical signal (representing vertical displacement) could be recorded directly on the X axis of an Electro-Instruments Model 420 X-Y recorder. A calibrated load cell in series with the specimen was used to measure load and was recorded on the Y axis of the same recorder.

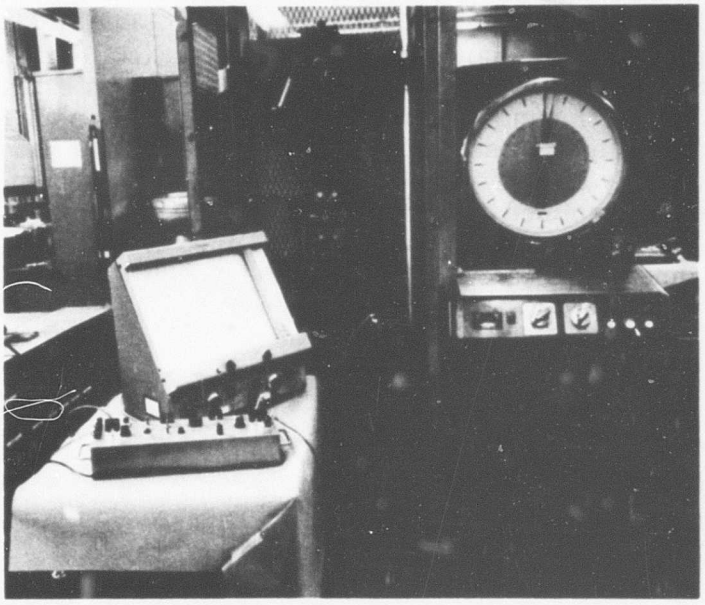

Figure 37. Fracture Toughness Test Setup.

Prior to testing, a calibration curve was constructed to correlate vertical displacement (v) measured by the compliance gage to crack extension in the specimen. Several specimens with initial crack lengths (2a) varying from zero to 3 inches were tested to determine their load-deflection curves under elastic loading conditions. From these results, a plot was drawn of Ev/S_g w (corrected specimen compliance term) versus π a/w (relative crack length term). A family of curves was then plotted by varying the modulus of elasticity (E) in the corrected specimen compliance term as shown in Figure 38.

The plane-strain fracture toughness (K_{Ic}) was calculated from the following equation:

$$E\,G_{Ic} = (1 - \mu^2)\,K_{Ic}^2 = S_g^2\,w \tan(\pi\,a/w)$$

The point of load deviation from linearity or the load-deflection curve was used as the load determination in the K_{Ic} calculation.

At the point of maximum load, the value of K_c, plane-stress fracture toughness, was calculated from the following equation:

$$E\,G_c = K_c^2 = S_g^2\,w \tan(\pi\,a/w)$$

Before the K_c calculation was made, the half-crack length (a) was determined from the compliance gage calibration curve, Figure 38. The corrected specimen compliance and the relative crack length were calculated for the point of load deviation. These quantities established a point on the calibration curve. If the point did not fall on one of the previously drawn lines, a new curve was established that had the same shape as the family of curves. From this curve and the calculated value of the corrected specimen compliance for the point of maximum load, the value of the relative crack length was determined and the plane-stress fracture toughness was calculated.

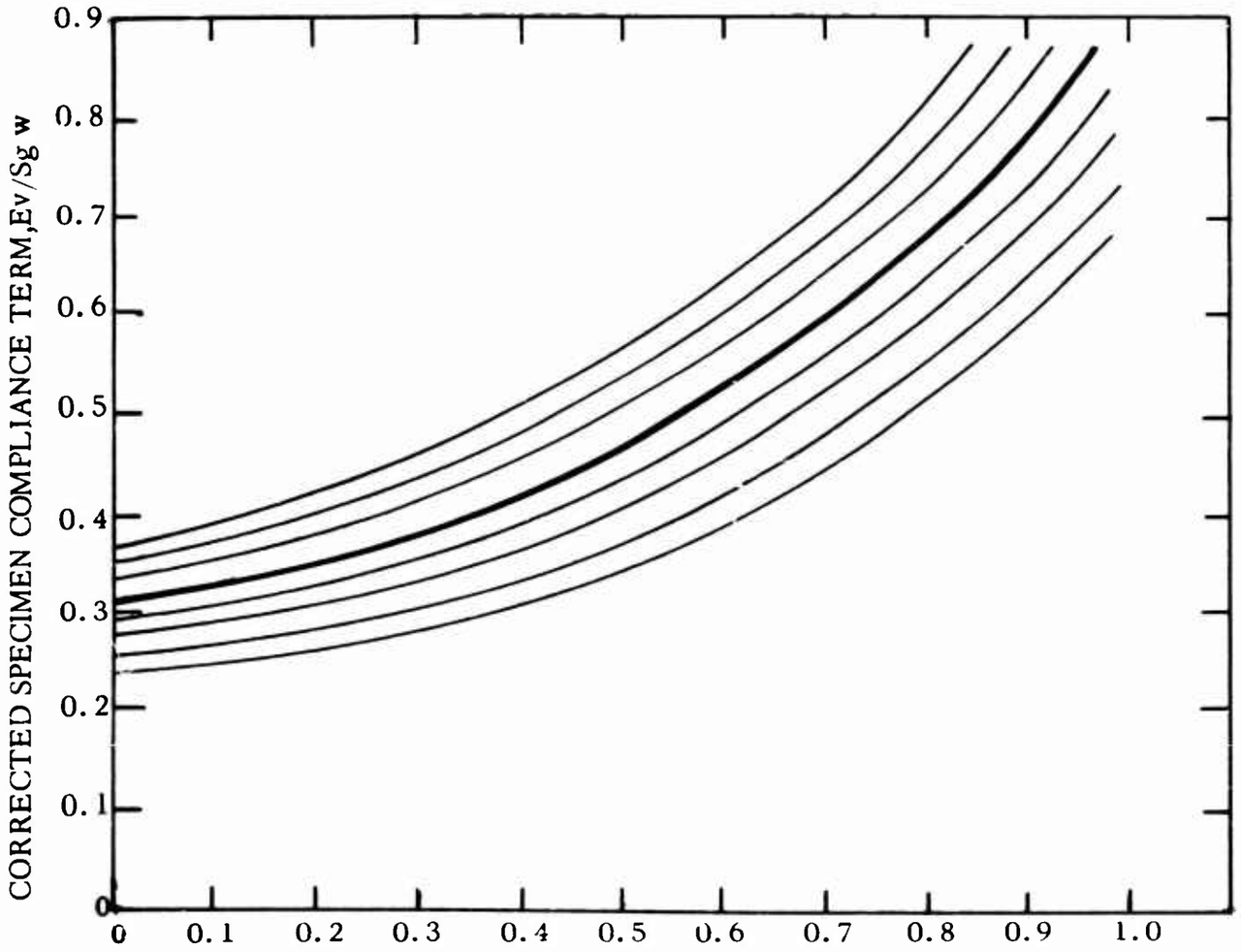

Figure 38. Compliance Gage Calibration Curves.

EXPERIMENTAL RESULTS AND DISCUSSION OF RESULTS

Tabulation of the plane-strain fracture toughness (K_{Ic}) and plane-stress fracture toughness (K_c) values for the two alloys tested are given in Table IV. Pop-in was observed in only a few specimens. Consequently, the K_{Ic} loads were taken at the point of load-deflection curve deviation from a straight line. Plane-strain fracture toughness values are considered to be conservatively low, since it is generally stated in the literature that pop-in occurs above the load-deflection-curve deviation point.

Brittle fracture of the specimens occurred before general yielding for both alloys, which allowed valid calculation of plane-stress fracture toughness values (K_c). Fracture toughness specimen failures are shown in Figure 39.

TABLE IV

FRACTURE TOUGHNESS TEST RESULTS

Material	Plane Strain (K_{Ic}) (psi $\sqrt{inch}$)	Plane Stress (K_c) (psi $\sqrt{inch}$)
Ti-6Al-6V-2Sn	42,300	69,400
Ti-13V-11Cr-3Al	45,800	81,200

Ti-6Al-6V-2Sn

Ti-13V-11Cr-3Al

Figure 39. Typical Fracture Surfaces for Fracture Toughness Specimens.

SECTION V - MAIN ROTOR CUFF TESTS AND COMPARISON OF THE CUFF RESULTS TO THE SMALL-SPECIMEN RESULTS

EXPERIMENTAL PROCEDURE

Helicopter main rotor cuffs, fabricated of Ti-6Al-6V-2Sn, Ti-13V-11Cr-3Al, Ti-6Al-4V,* and 4340 steel,* were fatigue tested on helicopter inboard main rotor blade specimens installed in a Sikorsky constant-displacement blade test machine. The test setup is shown in Figure 40.

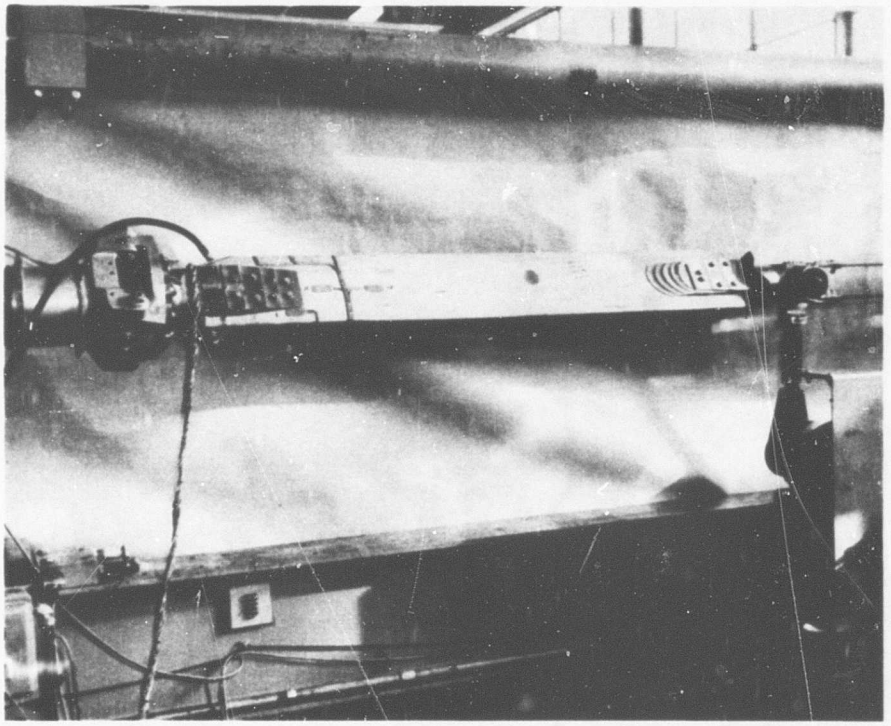

Figure 40. Main Rotor Blade Cuff Fatigue Test Setup.

*The tests on the Ti-6Al-4V (annealed condition, minimum ultimate tensile strength of 130,000 psi) and 4340 steel (heat-treated to 125,000-psi minimum ultimate tensile strength per MIL-H-6875) cuffs were not performed under the current contract, although the results are included in this report for comparative purposes.

A helicopter cuff is shown in Figure 41.

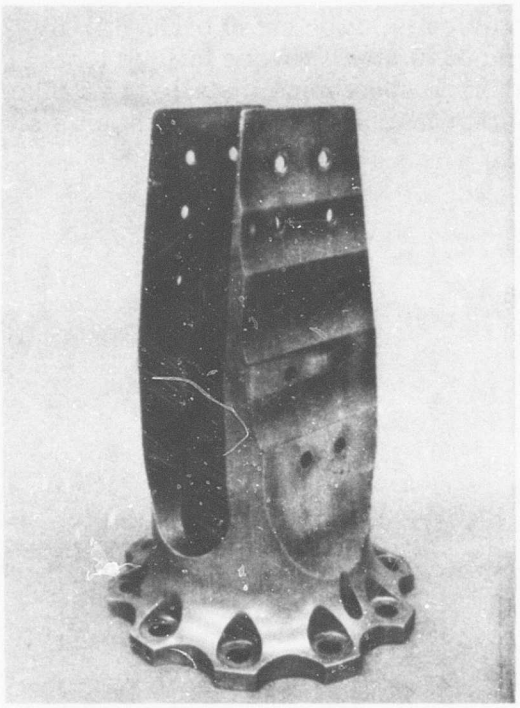

Figure 41. Helicopter Main Rotor Cuff.

Vibratory flatwise and edgewise bending loads were applied simultaneously by means of an eccentric crack arrangement, while simulated centrifugal loading was applied by compressed disc springs. The ratio of flatwise to edgewise vibratory loads and the magnitude of the centrifugal load closely simulated flight conditions. Vibratory loads were accelerated well above flight values to initiate fatigue cracks within a reasonable test time.

Each test specimen was instrumented with resistance strain gages. The gages were physically calibrated in terms of the applied load and were used to measure the vibratory load distribution. An Ellis Company Model BA-12 bridge amplifier and a cathode ray oscilloscope were used to read the vibratory loads. Centrifugal loadings were measured by calibrated load cells on the test machine and were verified by disc-spring deflection measurements. Microwire was installed in the critical areas of each cuff

specimen and was connected to the test machine motor control circuit so that a wire failure associated with fatigue crack initiation would stop the fatigue test.

Each specimen was tested in fatigue crack initiation followed by fatigue crack propagation testing. The crack initiation phase was performed at vibratory load levels well above flight conditions until cracks were detected either by visual inspection or by microwire.

Once fatigue cracks were generated, vibratory loads were reduced to levels simulating flight conditions. These levels were maintained until complete fracture of the cuff occurred. For these tests, cracks were considered to be detectable only when they had extended from the bolt-hole to the outer edge of the cuff plate, as shown in Figures 42 and 43.

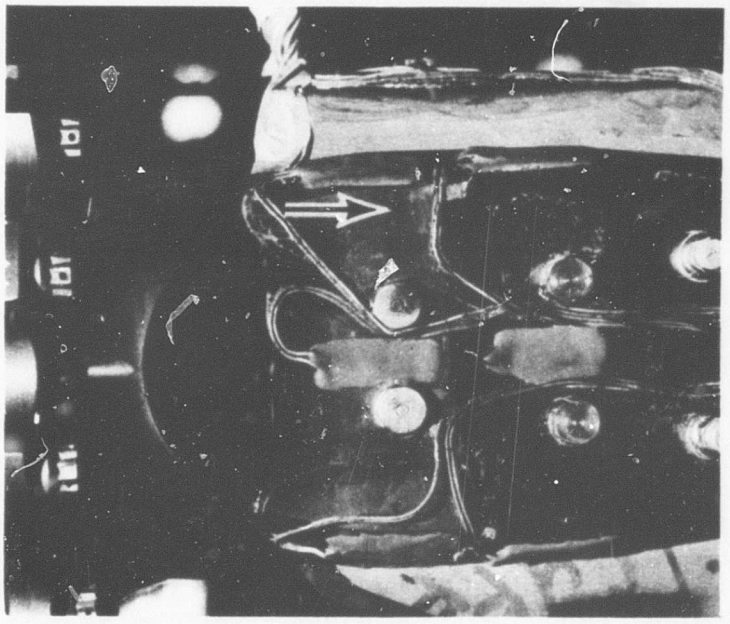

Figure 42. Typical Main Rotor Blade Cuff Fatigue Crack at Detection.

Note: Arrow indicates fatigue crack.

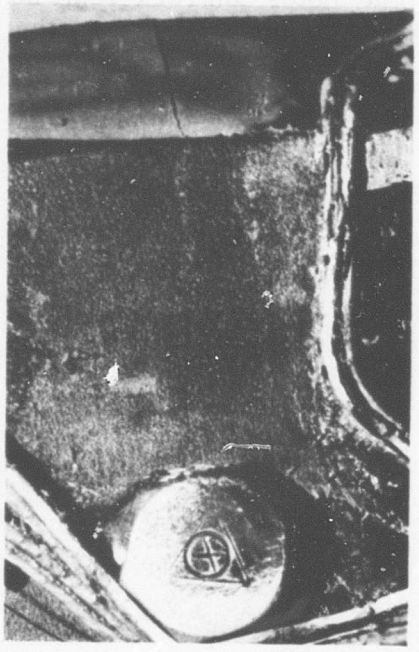

Figure 43. Enlargement of Fatigue Crack Area at Detection.

For the specific cuff configuration tested herein, the number of cycles during crack propagation is for hole-to-hole propagation prior to final fracture of the cuff. Figure 44 shows the complete fracture of a cuff.

The crack initiation S/N curve shapes used for Figures 45 through 48 are the same as those established from joint fatigue tests reported in Section II of this report.

EXPERIMENTAL RESULTS AND DISCUSSION OF RESULTS

Crack Initiation Tests

The results of the cuff crack initiation fatigue tests are summarized and ranked in order of mean strength in Table V. The vibratory stress used for the cuff fatigue evaluations is the sum of the flatwise and edgewise stress derived by dividing the flatwise and edgewise vibratory loads by theoretical section moduli at the inboard bolt-holes. These stress values were used to rate the cuff materials and are not comparable to the stress values listed for the small-size specimens. Figures 45 through 47 are plots of the test points and respective mean crack initiation curves for each material and bolt-hole condition. Figure 48 illustrates the relative mean strength of all materials and bolt-hole surface conditions tested.

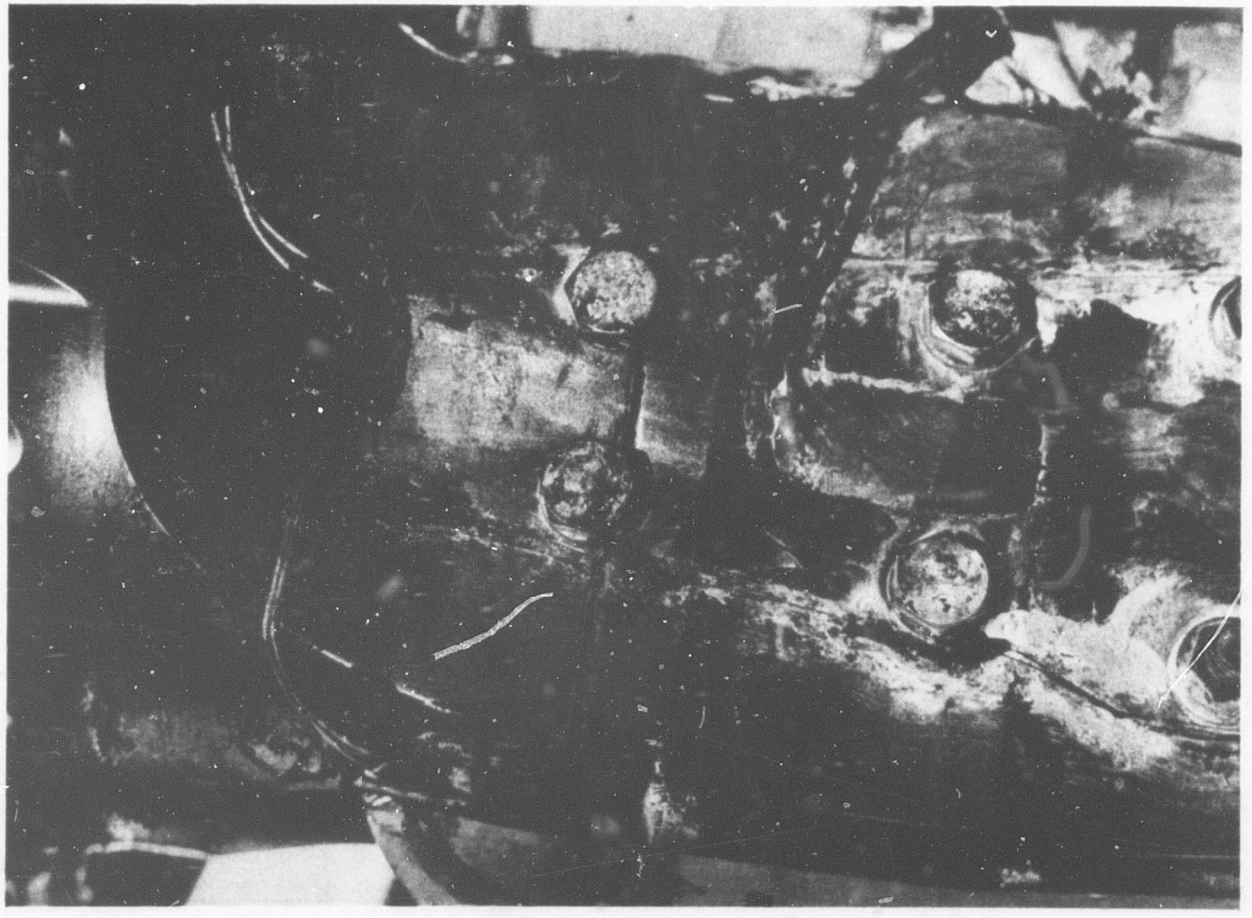

Figure 44. Typical Main Rotor Cuff Fatigue Fracture.

TABLE V

SUMMARY OF HELICOPTER CUFF CRACK INITIATION FATIGUE TEST RESULTS

Ranking	Material	Surface Condition @ Bolt-Holes	Number of Specimens	$\bar{X}$ (psi)*	s (psi)*	$s/\bar{X}$ (%)*	Mean Strength Relative to 4340 Steel Cuffs (%)
1	Ti-6Al-6V-2Sn	Expanded	4	6450	170	2.6	148
2	Ti-13V-11Cr-3Al	Expanded	1	5850	-	-	133
3	Ti-6Al-4V	Shot Peened	4	4900	470	9.5	113
4	4340 Steel	Reamed	13	4350	550	12.6	100
5	Ti-6Al-6V-2Sn	Reamed	2	3700	100	2.7	85
6	Ti-13V-11Cr-3Al	Reamed	3	2900	130	4.5	67

* Applicable at 10^8 cycles.

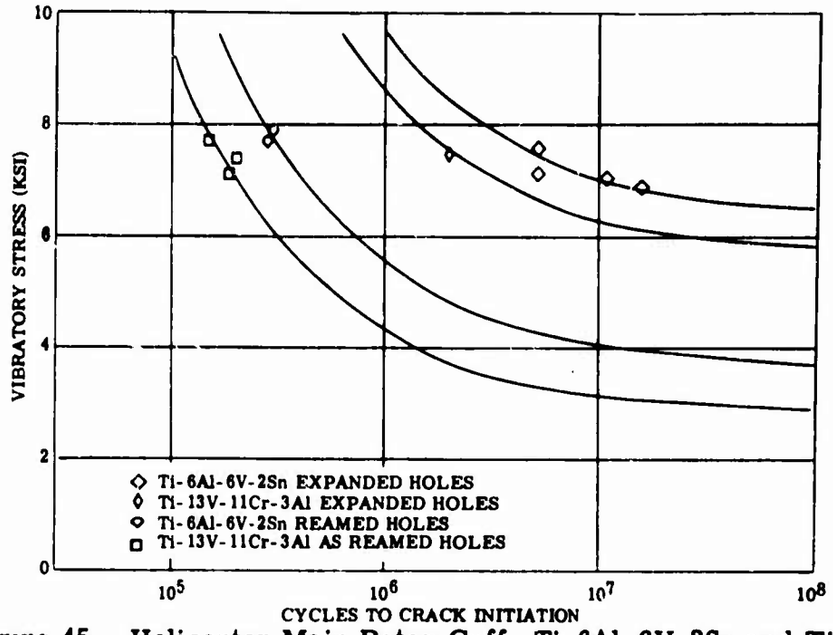

Figure 45. Helicopter Main Rotor Cuff, Ti-6Al-6V-2Sn and Ti-13V-11Cr-3Al, Vibratory Stress versus Cycles to Crack Initiation, Steady Centrifugal Load = 45,000 Pounds.

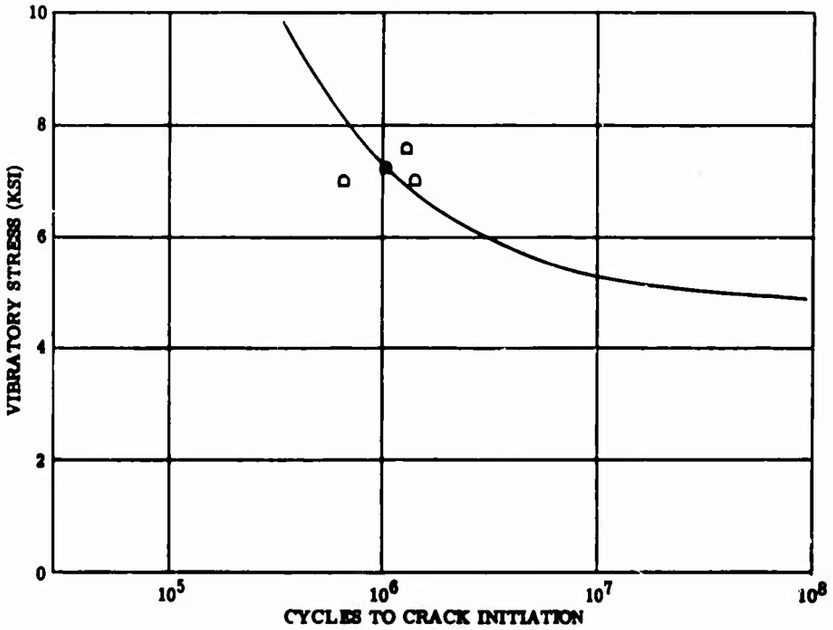

Figure 46. Helicopter Main Rotor Cuff, Ti-6Al-4V, Shot Peened Holes, Vibratory Stress versus Cycles to Crack Initiation, Steady Centrifugal Load = 45,000 Pounds.

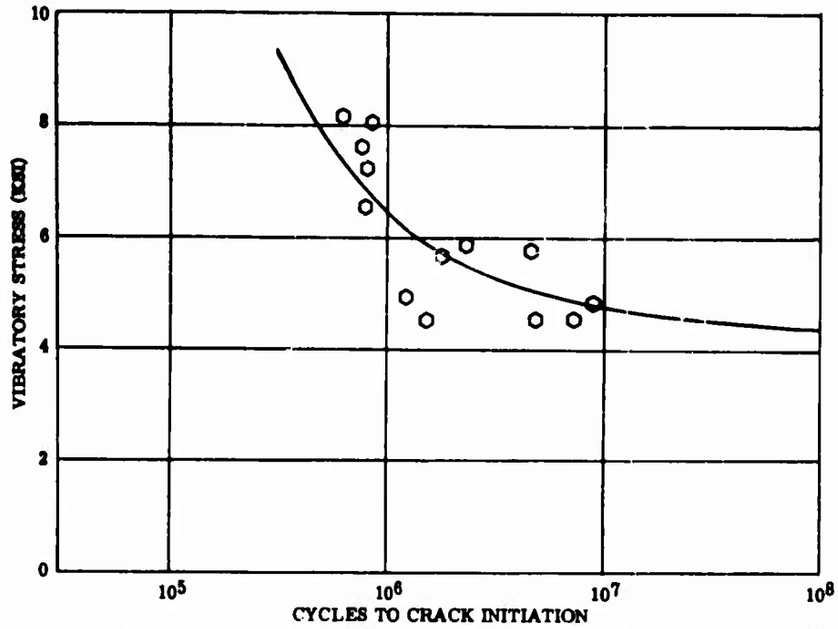

Figure 47. Helicopter Main Rotor Cuff, 4340 Steel, Reamed Holes, Vibratory Stress versus Cycles to Crack Initiation, Steady Centrifugal Load = 45,000 Pounds.

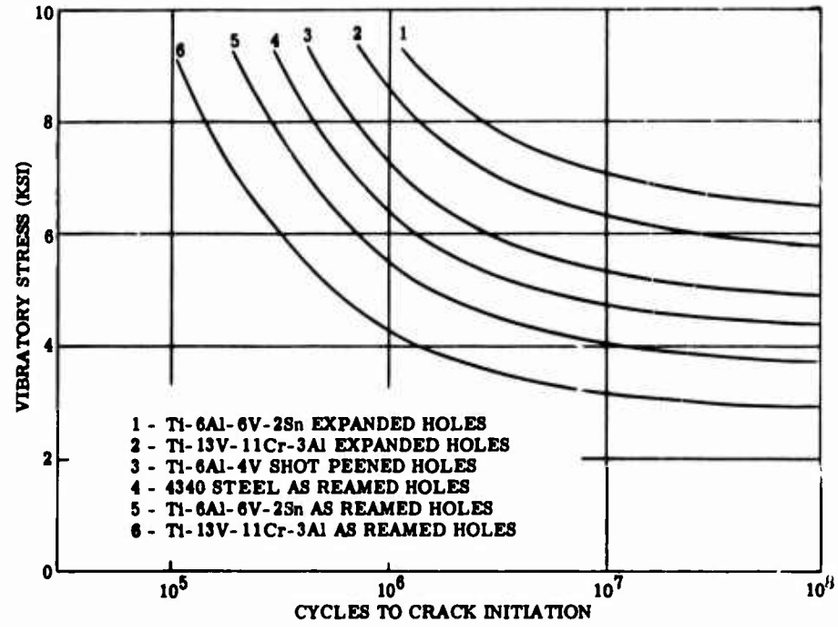

Figure 48. Helicopter Main Rotor Cuffs, Titanium Alloys and 4340 Steel, Vibratory Stress versus Cycles to Crack Initiation, Steady Centrifugal Load = 45,000 Pounds.

Table VI shows the improvement in crack initiation fatigue strength obtained by cold working the cuff-to-spar bolt-holes, in comparison to the results for the reamed bolt-holes, for both the Ti-6Al-6V-2Sn and the Ti-13V-11Cr-3Al alloys. The results in this table are based on both the small-specimen joint test and the cuff test data.

TABLE VI

COMPARATIVE CRACK INITIATION FATIGUE STRENGTH OF Ti-6Al-6V-2Sn AND Ti-13V-11Cr-3Al SPECIMENS WITH COLD-WORKED OR REAMED BOLT-HOLES

Specimen Type and Material	Mean Crack Initiation Fatigue Strength @ 10^8 for Various Bolt-Hole Conditions (psi)		Fatigue Strength Ratio
	Reamed	Expanded	Expanded/Reamed
Joint Specimens (Section II):			
Ti-6Al-6V-2Sn	4800	10200	2.1
Ti-13V-11Cr-3Al	4400	8400	1.9
Full-Size Cuffs:			
Ti-6Al-6V-2Sn	3700	6450	1.7
Ti-13V-11Cr-3Al	2900	5800	2.0

Crack Propagation Tests

Results of cuff fatigue crack propagation tests are plotted in Figure 49. The materials with the best fatigue crack propagation resistance appeared to be Ti-6Al-6V-2Sn with expanded holes and 4340 steel with reamed holes. The results indicate that the crack propagation resistance of Ti-6Al-6V-2Sn (expanded, 4) and 4340 steel (reamed, 13) is comparable. The terms in brackets refer to the bolt-hole condition and the number of specimens respectively. The results for the remaining cuff alloys with various bolt-hole conditions, in order of decreasing crack propagation resistance, were estimated to be as follows: Ti-6Al-4V (shot peened, 4) and Ti-6Al-6V-2Sn (reamed, 2), Ti-13V-11Cr-3Al (reamed, 3), Ti-13V-11Cr-3Al (expanded, 1).

In all cases, fatigue cracks originated at the bolt-holes. Figures 50 and 51 show typical fracture surfaces for the Ti-6Al-6V-2Sn and Ti-13V-11Cr-3Al cuffs.

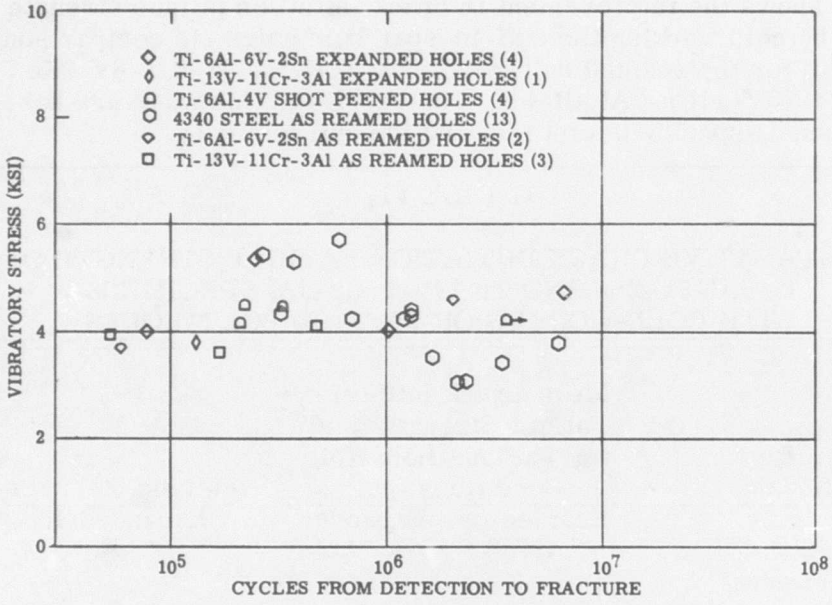

Figure 49. Helicopter Main Rotor Cuffs, Titanium Alloys and 4340 Steel, Vibratory Stress versus Cycles From Crack Detection to Fracture, Steady Centrifugal Load = 45,000 Pounds.

Figure 50. Typical Fracture Surface for Ti-6Al-6V-2Sn Cuff.

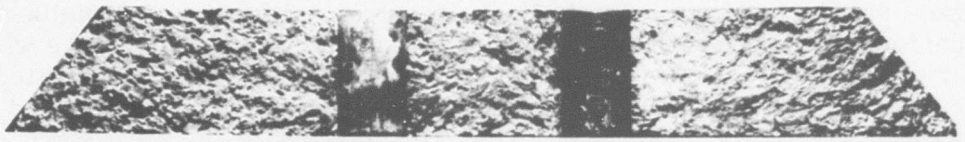

Figure 51. Typical Fracture Surface for Ti-13V-11Cr-3Al Cuff.

CONCLUSIONS

For the alloys and heat treatments tested - Ti-6Al-6V-2Sn and Ti-13V-11Cr-3Al solution heat treated and aged, Ti-6Al-4V annealed, and 4340 steel heat treated to a 125-ksi minimum ultimate tensile strength - it is concluded that:

1. The fatigue crack initiation strength of Ti-6Al-6V-2Sn is superior to that of Ti-13V-11Cr-3Al on the basis of both small-specimen and full-size component tests.

2. The fatigue crack propagation resistance for small-size specimens of Ti-6Al-6V-2Sn and Ti-13V-11Cr-3Al is not significantly different.

3. Fracture toughness properties of Ti-6Al-6V-2Sn are comparable to those of Ti-13V-11Cr-3Al.

4. The titanium alloy and the steel cuffs with various bolt-hole conditions are ranked as follows, in order of decreasing crack initiation strength: Ti-6Al-6V-2Sn (expanded), Ti-13V-11Cr-3Al (expanded), Ti-6Al-4V (shot peened), 4340 steel (reamed), Ti-6Al-6V-2Sn (reamed), and Ti-13V-11Cr-3Al (reamed). Since some of these full-scale test results are based on a limited number of specimens, observed differences may not be statistically significant.

5. Both full-scale cuff tests and joint tests of small-size specimens indicate that the crack initiation strength of Ti-6Al-6V-2Sn and Ti-13V-11Cr-3Al are improved approximately 2:1 by cold working the bolt-holes. Expanding the reamed holes resulted in a greater improvement in the endurance strength over that achieved by shot-peening the holes.

6. The results indicate that the crack propagation resistance of Ti-6Al-6V-2Sn expanded, 4340 steel reamed, Ti-6Al-4V shot peened, and Ti-6Al-6V-2Sn reamed is of the same order. Cuffs of Ti-13V-11Cr-3Al expanded and reamed show a trend toward lower resistance to fatigue crack propagation; however,these results are based on a limited number of specimens and observed differences are not statistically significant.

RECOMMENDATIONS

1. Investigate the practicability of employing Ti-6Al-6V-2Sn for helicopter applications in a salt-water environment. Determine the influence of salt solutions on fatigue crack propagation and fracture toughness behavior.

2. Investigate the influence of forging above the beta transus on the fatigue crack initiation, crack propagation, and fracture toughness properties of Ti-6Al-4V and Ti-6Al-6V-2Sn.

3. Ti-13V-11Cr-3Al is a heat-treatable material which can be heat-treated to very high yield strength values for titanium alloys. Conduct an investigation to determine the influence of heat-treatment conditions (especially solution heat-treatment temperature) on the fatigue crack initiation properties.

4. Since cold working the holes resulted in an improvement in the joint strength of bolted titanium alloy specimens, this effect should be further investigated. Determine the influence of expanding (roller burnishing and bearingizing) and shot peening on fatigue crack initiation in other useful materials (various steels, aluminum, and additional titanium alloys).

5. The fatigue crack propagation and fracture toughness ratings of materials are influenced by various factors, including surface condition, grain structure, stress level and specimen size. Investigate the effect of specimen dimensions on fatigue crack propagation and fracture toughness in materials of interest.

BIBLIOGRAPHY

1. Boyle, R., "A Method for Determining Crack Growth," Materials Research and Standards, Volume 2, No. 8, August 1962, pp. 646-651.

2. Degnan, W. G., Dripchak, P. D., Matusovich, C. J., "Fatigue Crack Propagation in Aircraft Materials," USAAVLABS Technical Report 66-9, U. S. Army Aviation Materiel Laboratories, Fort Eustis, Virginia, March 1966.

3. Federal Test Method Standard No. 151a, Method 211.1, Tension Test, May 6, 1959.

4. Fracture Toughness Testing and Its Applications, ASTM Special Technical Publication No. 381, American Society for Testing and Materials, Philadelphia, Pa., 1965.

5. Heywood, R. D., "The Strength of Lugs in Fatigue," Royal Aircraft Establishment Technical Note Structures 182, Ministry of Supply, London, W. C. 2, January 1956.

APPENDIX
MATERIAL CHEMICAL ANALYSIS, TENSILE STRENGTH AND FORGING METHODS

SECTION I - AXIAL TENSION-TENSION FATIGUE TEST SPECIMENS

The initial bar forging stock (3-3/4-inch round-cornered square) was supplied by Titanium Metals Corporation of America (TMCA) for both alloys. Tables VII and VIII list TMCA's chemical analysis of the material supplied and the chemical analysis of the forging vendor, Wyman-Gordon Company (WG).

TABLE VII

CHEMICAL ANALYSIS OF Ti-6Al-6V-2Sn

Analysis Source	C	Fe	N	Al	V	H	O	Sn	Cu	Ti
Heat Number D-6423 Beta Transus 1650° F										
TMCA	.022	.82	.016	5.5	5.7	.003	.10	2.0	.76	bal.
TMCA	.026	.68	.018	5.4	5.7	-	-	2.0	.62	bal.
WG	.012	.86	.015	5.6	5.6	.003	.115	2.0	.79	bal.

TABLE VIII

CHEMICAL ANALYSIS OF Ti-13V-11Cr-3Al

Analysis Source	C	Fe	N	Al	V	H	O	Cr	Ti
Heat Number D-6999									
TMCA	.029	.18	.019	3.0	13.4	.009	.12	11.3	bal.
TMCA	.028	.16	.026	3.1	13.4	-	-	11.0	bal.
WG	.021	.15	.025	2.8	13.6	.007	.12	11.2	bal.

The Ti-6Al-6V-2Sn forging bar stock was heated to 1625° F for 2 hours before the first forging operation, was returned to the furnace at the

same temperature for 1 hour before sizing to final dimensions, and was water quenched. The finished forging was solution heat-treated at 1550° F for 1 hour, water quenched, aged at 1050° F for 4 hours, and air cooled.

The time-temperature conditions for this heat treatment were determined by preliminary time-temperature-tension test experiments on specimen blanks cut from the forging to determine the optimum heat treatment conditions prior to heat treating the finished forgings. The minimum desired ultimate tensile strength was 165,000 psi. Table IX lists the tensile properties obtained (longitudinal direction) on the finished forging for this alloy. These tensile tests and all other tensile test results reported were performed in accordance with Federal Test Method Standard 151a, Method 211.1, with a type R-3 specimen, Reference 3.

TABLE IX

TENSILE PROPERTIES OF Ti-6Al-6V-2Sn

	F_{tu} (psi)	F_{ty} (psi)	e (%)	R.A. (%)
	171,000	162,000	8.5	25.1
	172,000	162,000	7.0	16.6
	171,000	163,000	8.5	18.8
	170,000	161,000	10.0	21.7
Average -	170,800	162,000	8.5	20.5

The Ti-13V-11Cr-3Al forging bar stock was heated to 1700° F for 2-1/2 hours before the first forging operation, was returned to the furnace at the same temperature for 1 hour before sizing to final dimensions, and was air cooled. The finished forging was solution heat-treated at 1335° F for 1 hour, air cooled, reheated to 1450° F for 1/2 hour, fan cooled, aged at 900° F for 20 hours, and air cooled. The temperatures and times listed in this heat treatment were determined on capability tests prior to heat treating the finished forgings to obtain a minimum ultimate tensile strength of 175,000 psi. Table X lists the tensile properties obtained (longitudinal direction) on the finished forging for this alloy.

Photomicrographs indicating the structure of the finished forgings of both alloys are shown in Figures 52 and 53. This structure is not

considered to be optimum by the forging vendor because of the relatively small amount of reduction (29%), the short heating time at forging temperature, and the possible retention of the structure of the original bar. This condition could be present in a normal forging.

TABLE X

TENSILE PROPERTIES OF Ti-13V-11Cr-3Al

	F_{tu} (psi)	F_{ty} (psi)	e (%)	R.A. (%)
	182,000	170,000	6.0	9.3
	183,000	168,000	7.0	10.8
	181,000	170,000	8.5	12.3
	180,000	168,000	9.2	10.0
Average -	181,500	169,000	7.7	10.6

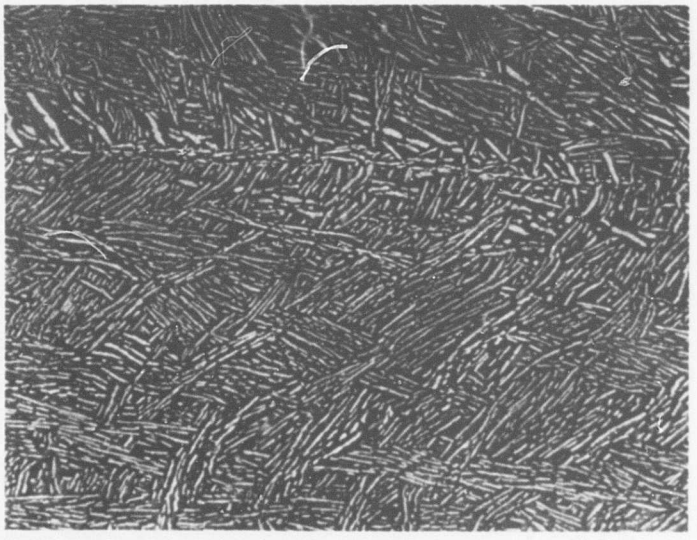

Figure 52. Photomicrograph of Ti-6Al-6V-2Sn Axial Fatigue Specimen.

Note: Magnification 200X, Etchant HNO_3 + HF.

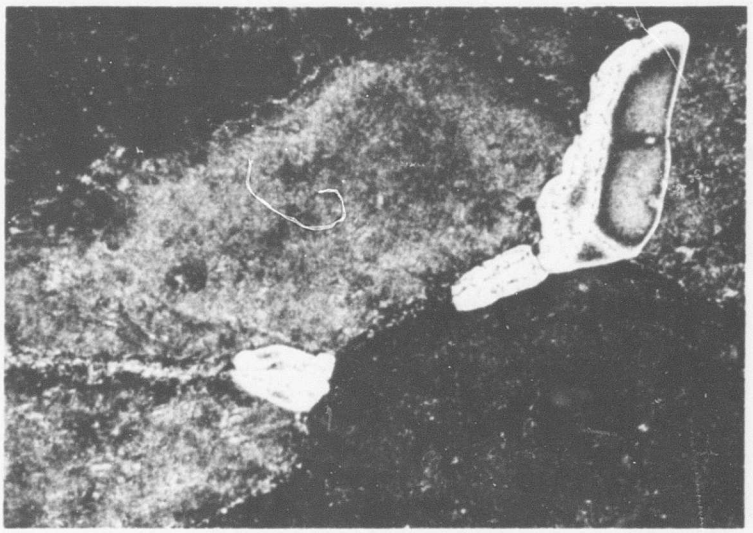

Figure 53. Photomicrograph of Ti-13V-11Cr-3Al Axial Fatigue Specimen.

Note: Magnification 200X, Etchant HNO_3 + HF.

SECTION II - JOINT FATIGUE TEST SPECIMENS

The initial bar forging stock (3-inch round-cornered square) was supplied by Titanium Metals Corporation of America (TMCA) for both alloys. Tables XI and XII list the material supplier's chemical analysis of both materials and the chemical analysis of the forging vendor, Wyman-Gordon Company (WG).

TABLE XI

CHEMICAL ANALYSIS OF Ti-6Al-6V-2Sn

Analysis Source	C	Fe	N	Al	V	H	O	Sn	Cu	Ti
Heat Number D-7804 Beta Transus 1640° F										
TMCA	.020	.79	.014	5.7	5.5	.007	.11	2.0	.73	bal.
TMCA	.022	.70	.015	5.9	5.5	-	-	2.0	.65	bal.
WG	.016	.85	.012	5.7	5.6	.004	.12	2.0	.85	bal.

TABLE XII

CHEMICAL ANALYSIS OF Ti-13V-11Cr-3Al

Analysis Source	C	Fe	N	Al	V	H	O	Cr	Ti
Heat Number D-7590									
TMCA	.018	.16	.029	3.1	13.6	.003	.13	10.6	bal.
TMCA	.018	.16	.027	3.0	13.5	.008	.13	10.6	bal.
WG	.015	.14	.036	3.2	13.4	.009	.13	10.5	bal.

The Ti-6Al-6V-2Sn forging bar stock was heated to 1625° F for 3 hours before the first forging operation, was returned to the furnace at the same temperature for 1 hour before sizing to final dimensions, and was water quenched. The finished forging was solution heat-treated at 1550° F for 1 hour, water quenched, aged at 1100° F for 4 hours, and air cooled. The time-temperature conditions for this heat treatment were determined by preliminary time-temperature-tension test experiments prior to the heat treating of the finished forgings. The minimum desired ultimate tensile strength was 165,000 psi. Table XIII lists the tensile properties obtained on the finished forgings for this alloy. Tensile tests were made in the longitudinal direction of the forging.

TABLE XIII

TENSILE PROPERTIES OF Ti-6Al-6V-2Sn

	F_{tu} (psi)	F_{ty} (psi)	e (%)	R.A. (%)
	164,000	161,000	13.5	44.4
	164,000	159,000	15.5	50.0
	180,000	172,000	10.5	26.6
	168,000	166,000	14.5	47.2
Average -	169,000	164,500	13.5	42.0

The Ti-13V-11Cr-3Al forging bar stock was heated to 1700° F for 2 hours before the first forging operation, was returned to the furnace at the same temperature for 1 hour before sizing to final dimensions, and was air cooled. The finished forging was solution heat-treated at 1335° F for 1 hour, air cooled, reheated to 1450° F for 1/2 hour, fan cooled, aged at 900° F for 15 hours, and air cooled. This heat treatment was determined on the basis of preliminary time-temperature-tension tests prior to heat treating the finished forgings. The tests were aimed at obtaining minimum ultimate tensile strengths of 175,000 psi. Table XIV lists the tensile properties obtained on the finished forging for this alloy. All tensile tests were taken in the longitudinal direction of the forging.

Photomicrographs indicating the structure obtained in the finished forgings of both alloys are shown in Figures 54 and 55. The structures obtained for these forgings were considered to be better than the structures obtained for the axial tension-tension fatigue specimens. Forging reduction for the joint specimen forgings was 37.5%.

TABLE XIV

TENSILE PROPERTIES OF Ti-13V-11Cr-3Al

	F_{tu} (psi)	F_{ty} (psi)	e (%)	R.A. (%)
	182,000	171,000	5.5	11.6
	180,000	169,000	6.0	12.2
	190,000	178,000	6.0	10.0
	194,000	182,000	6.0	7.8
Average -	186,500	175,000	5.9	10.4

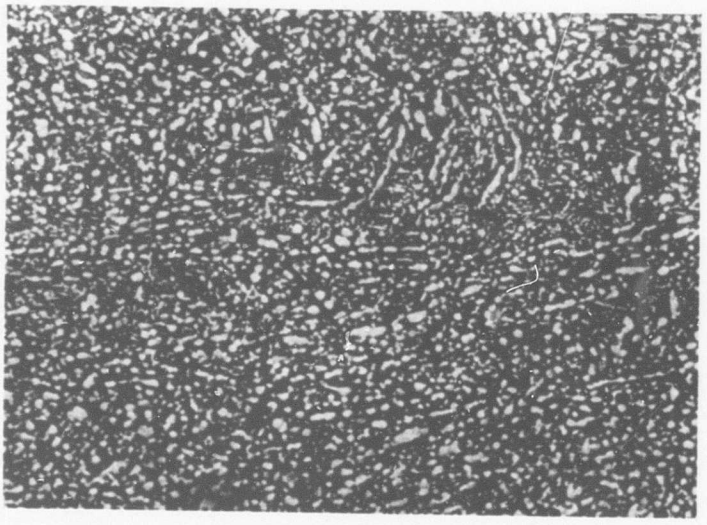

Figure 54. Photomicrograph of Ti-6Al-6V-2Sn Joint Fatigue Specimen.

Note: Magnification 200X, Etchant HNO_3 + HF.

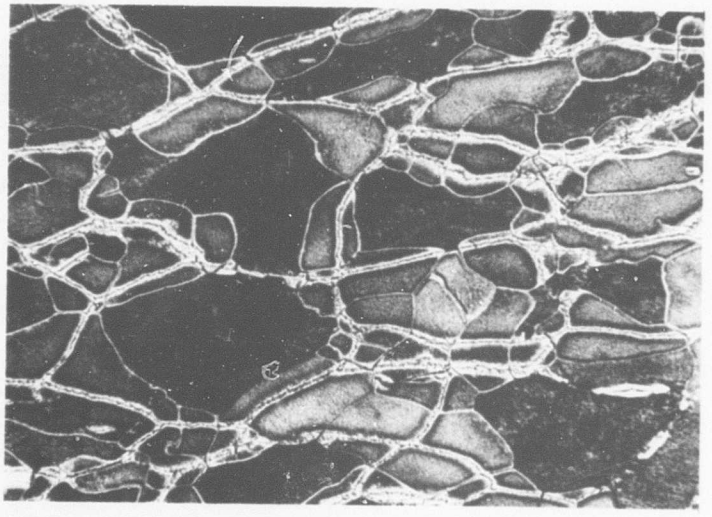

Figure 55. Photomicrograph of Ti-13V-11Cr-3Al Joint Fatigue Specimen.

Note: Magnification 200X, Etchant HNO_3 + HF.

SECTION III - FATIGUE CRACK PROPAGATION AND FRACTURE TOUGHNESS TEST SPECIMENS.

The initial bar forging stock (2-inch round-cornered square) was supplied by Titanium Metals Corporation of America (TMCA) for both alloys. Tables XV and XVI list the chemical analysis of the material supplier and of the forging vendor, Wyman-Gordon Company (WG).

TABLE XV

CHEMICAL ANALYSIS OF Ti-6Al-6V-2Sn

Analysis Source	C	Fe	N	Al	V	H	O	Sn	Cu	Ti
Heat Number D-7804 Beta Transus 1640° F										
TMCA	.020	.79	.014	5.7	5.5	.007	.11	2.0	.73	bal.
TMCA	.022	.70	.015	5.9	5.5	-	-	2.0	.65	bal.
WG	.016	.85	.012	5.7	5.6	.004	.12	2.0	.85	bal.

TABLE XVI

CHEMICAL ANALYSIS OF Ti-13V-11Cr-3Al

Analysis Source	C	Fe	N	Al	V	H	O	Cr	Ti
Heat Number D-5769									
TMCA	.025	.15	.030	3.1	13.6	.007	.13	11.2	bal.
TMCA	.022	.12	.033	3.1	13.6	-	-	11.0	bal.
WG	.018	.17	.028	2.8	13.7	.009	.13	11.2	bal.

The Ti-6Al-6V-2Sn forging bar stock was heated to 1625° F for 2 hours before the first forging operation, was returned to the furnace at the same temperature for 1/2 hour before sizing to final dimensions, and was water quenched. The forging was reheated to 1625° F for 2 hours, flattened, and water quenched. The finished forging was solution heat-treated at 1650° F for 1 hour, water quenched, aged at 1200° F for 2 hours, and air cooled. Tensile properties obtained for this alloy are listed in

Table XVII. Tensile specimens were tested in both the longitudinal and the transverse direction of the forging. The time-temperature conditions employed for this heat treatment were determined by time-temperature-tension tests prior to heat treating the finished forgings. The minimum desired ultimate tensile strength was 165,000 psi.

TABLE XVII

TENSILE PROPERTIES OF Ti-6Al-6V-2Sn

F_{tu} (psi)	F_{ty} (psi)	e (%)	R.A. (%)	Direction
181,000	173,000	8.0	20.3	longitudinal
180,000	170,000	9.0	23.7	longitudinal
184,000	174,000	6.5	13.0	transverse
181,000	169,000	7.5	14.4	transverse

The Ti-13V-11Cr-3Al forging bar stock was heated to 1800° F for 2 hours before the first forging operation, was returned to the furnace at the same temperature for 1 hour before sizing to final dimensions, and was air cooled. The forging was reheated to 1800° F for 2 hours, flattened, and air cooled. The finished forging was solution heat-treated at 1335° F for 1 hour, air cooled, reheated to 1450° F for 1/2 hour, water quenched, aged at 900° F for 16 hours, and air cooled. Tensile properties obtained from this forging are listed in Table XVIII. Tensile specimens were tested in the longitudinal and transverse directions of the forging. The time-temperature conditions for this heat treatment were determined by time-temperature-tension tests prior to heat treating the finished forgings. The desired ultimate tensile strength (minimum) was 175,000 psi.

TABLE XVIII

TENSILE PROPERTIES OF Ti-13V-11Cr-3Al

F_{tu} (psi)	F_{ty} (psi)	e (%)	R.A. (%)	Direction
197,000	182,000	7.0	9.3	longitudinal
195,000	178,000	7.0	13.0	longitudinal
190,000	176,000	6.5	15.2	transverse
185,000	171,000	7.0	16.0	transverse

Photomicrographs showing the structure obtained on the finished forgings of both alloys are presented in Figures 56 and 57. The forging reduction was 72% for these specimens.

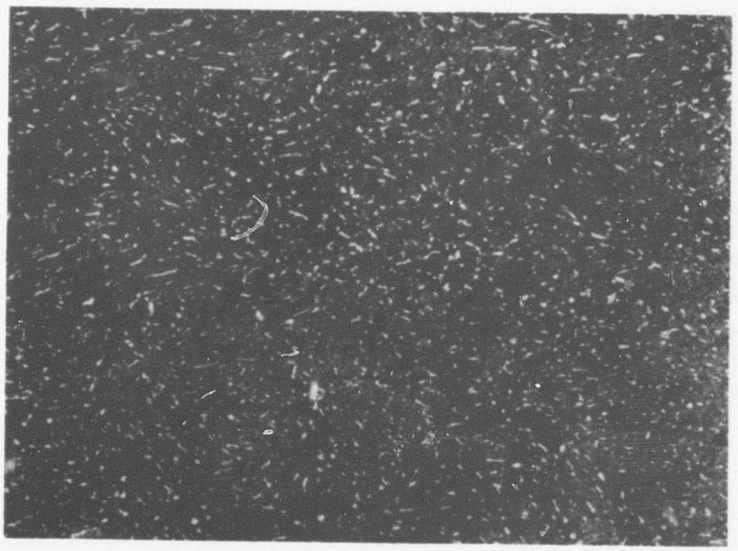

Figure 56. Photomicrograph of Crack Propagation Specimen, Ti-6Al-6V-2Sn.

Note: Magnification 200X, Etchant HNO_3 + HF.

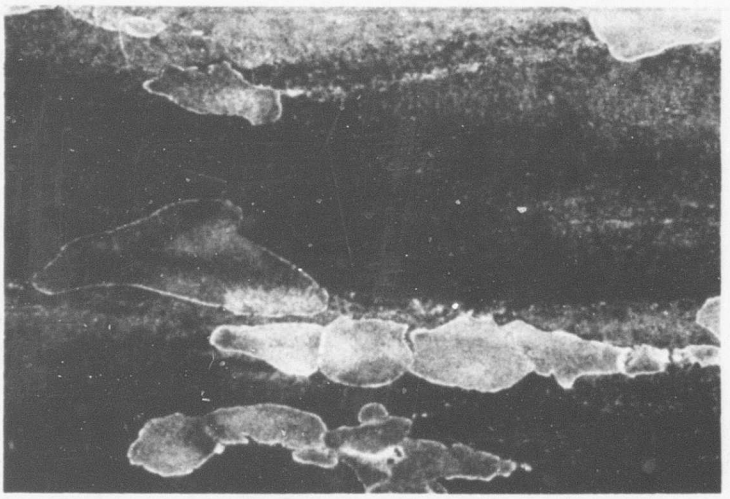

Figure 57. Photomicrograph of Crack Propagation Specimen, Ti-13V-11Cr-3Al.

Note: Magnification 200X, Etchant HNO_3 + HF.

SECTION IV - CUFF FATIGUE TEST SPECIMENS

The initial forging stock (6-inch-round and 8-1/4-inch-round billets) was supplied by Titanium Metals Corporation of America (TMCA) for both alloys. The 8-1/4-inch-round stock was used for the two additional Ti-6Al-6V-2Sn cuffs required for the supplementary contract, since 6-inch-round stock was not available at the time. Tables XIX and XX list TMCA's chemical analysis and the chemical analysis of the forging vendor, Wyman-Gordon Company (WG). Separate analyses are presented for the original four Ti-6Al-6V-2Sn cuffs and the two additional cuffs under the supplementary contract.

TABLE XIX

CHEMICAL ANALYSIS OF Ti-6Al-6V-2Sn CUFF FORGINGS

Analysis Source	C	Fe	N	Al	V	H	O	Sn	Cu	Ti
(A) Original Four Cuffs Heat Number D-6423 Beta Transus 1650° F										
TMCA	.022	.82	.016	5.5	5.7	.003	.10	2.0	.76	bal.
TMCA	.026	.68	.018	5.4	5.7	-	-	2.0	.62	bal.
WG	.012	.86	.015	5.6	5.6	.003	.115	2.0	.79	bal.
(B) Two Additional Cuffs Heat Number G-68 Beta Transus 1705° F										
TMCA	.022	.73	.013	5.6	5.7	.004	.16	1.9	.70	bal.
TMCA	.026	.60	.014	5.7	5.6	-	-	1.8	.55	bal.
TMCA	.022	.61	.014	5.6	5.4	.008	.19	1.9	.58	bal.
WG	.018	.68	.012	5.7	5.4	.005	.16	2.1	.60	bal.

TABLE XX

CHEMICAL ANALYSIS OF Ti-13V-11Cr-3Al CUFF FORGINGS

Analysis Source	C	Fe	N	Al	V	H	O	Cr	Ti
Heat Number D-7641									
TMCA	.028	.17	.023	3.0	13.6	.008	.15	11.2	bal.
TMCA	.025	.16	.024	3.1	13.8	.008	.15	11.3	bal.
WG	.018	.12	.039	3.2	13.1	.006	.14	10.4	bal.

Table XXI gives the forging operations, temperatures, times,and cooling methods employed in forging the Ti-6Al-6V-2Sn cuffs. Figure 58 shows the configuration of the cuffs after the final forging operation.

TABLE XXI

Ti-6Al-6V-2Sn CUFF FORGING PROCEDURE

Forging Operation	Heat Cycles-Hrs.	Furnace Temp. °F	Method of Cooling
Upset Forge	2-1/2	1625	Air cool to room temp.
Flatten	2-1/2	1625	Air cool to room temp.
1st Finish	2-1/2	1625	Reheat immediately
2nd Finish	1	1625	Water quench

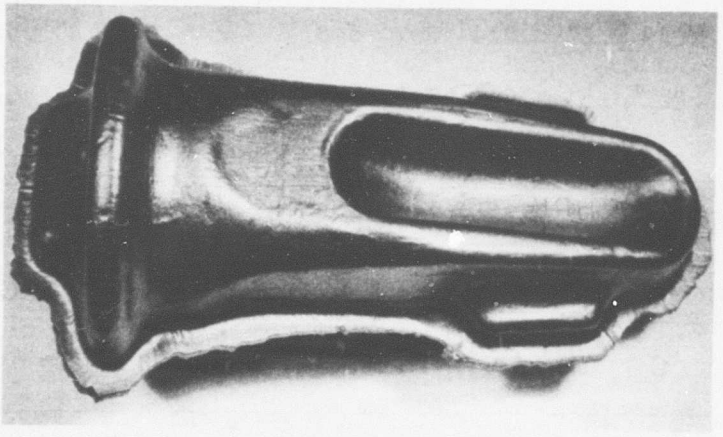

Figure 58. Titanium Cuff After Final Forging Operation.

The forging procedure for the two additional cuffs was the same as outlined above with the following two exceptions:

1. All forging operations were performed at 1675° F.

2. A preliminary operation of drawing down the stock from 8-1/2 inches to 6 inches was required.

The finished forgings were solution heat-treated at 1550° F for 1 hour, water quenched, aged at 1100° F for 4 hours, and air cooled. The two additional forgings were heat treated in the same manner except that the solution heat treatment temperature was 1600° F.

The time-temperature conditions for the heat treatments were determined by heat treatment-tension test studies prior to heat treating the finished forgings. The minimum desired ultimate tensile strength was 165,000 psi. Table XXII lists the tensile properties in the longitudinal and transverse directions obtained, employing test coupons from each forging.

TABLE XXII

TENSILE PROPERTIES OF Ti-6Al-6V-2Sn CUFFS

	LONGITUDINAL				TRANSVERSE			
	F_{tu} (ksi)	F_{ty} (ksi)	e (%)	R.A. (%)	F_{tu} (ksi)	F_{ty} (ksi)	e (%)	R.A. (%)
	171	162	13.5	45.1	171	162	13.0	40.1
	172	164	13.0	41.7	176	166	14.0	43.1
	178	168	12.5	40.1	178	167	12.0	40.1
	170	160	12.0	37.6	174	166	13.0	41.7
	175	164	12.0	38.2	172	162	13.0	43.1
Average	173.2	163.6	12.6	40.5	174.2	164.6	13.0	41.6
Additional Cuffs								
	178	169	10.0	35.7	178	169	10.5	53.5
	179	171	10.0	32.7	178	172	12.0	44.4
Average	178.5	170.0	10.0	34.2	178.0	170.5	11.3	49.0

Table XXIII gives the forging operations, temperatures, and times in forging the Ti-13V-11Cr-3Al cuffs. The finished forgings were heat treated at 1335° F for 1 hour, air cooled, solution treated at 1450° F for 1 hour, air cooled, and aged at 900° F for 11 to 15 hours. The temperatures and times listed in this heat treatment were determined by

heat treatment time-temperature-tension test studies prior to heat treating the finished forgings to obtain a minimum ultimate strength of 175,000 psi.

TABLE XXIII

Ti-13V-11Cr-3Al CUFF FORGING PROCEDURE

Forging Operation	Heat Cycles-Hrs.	Furnace Temp. °F	Method of Cooling
Upset Forge	2-1/2	1800	Air cool
Flatten	2-1/2	1800	Air cool
1st Finish	2-3/4	1700	Reheat immediately
2nd Finish	1	1700	Air cool

Table XXIV lists the tensile properties in the longitudinal and transverse directions obtained, employing test coupons from each forging.

TABLE XXIV

TENSILE PROPERTIES OF Ti-13V-11Cr-3Al CUFFS

	LONGITUDINAL				TRANSVERSE			
	F_{tu} (ksi)	F_{ty} (ksi)	e (%)	R.A. (%)	F_{tu} (ksi)	F_{ty} (ksi)	e (%)	R.A. (%)
	180	166	4.5	9.3	175	167	3.5	4.7
	184	172	5.0	7.8	181	168	4.0	6.2
	182	170	4.5	6.2	177	164	3.0	6.2
	179	168	2.5	7.0	179	168	3.0	7.0
	188	170	5.0	7.8	188	165	5.0	7.8
Average	182.6	169.2	4.3	7.6	180.0	166.4	3.7	6.4

One cuff forging of each alloy was sectioned to observe the uniformity of tensile properties throughout all sections. Figures 59 and 60 show the test specimen locations in the Ti-6Al-6V-2Sn and Ti-13V-11Cr-3Al cuffs. Tensile test results are given in Tables XXV and XXVI.

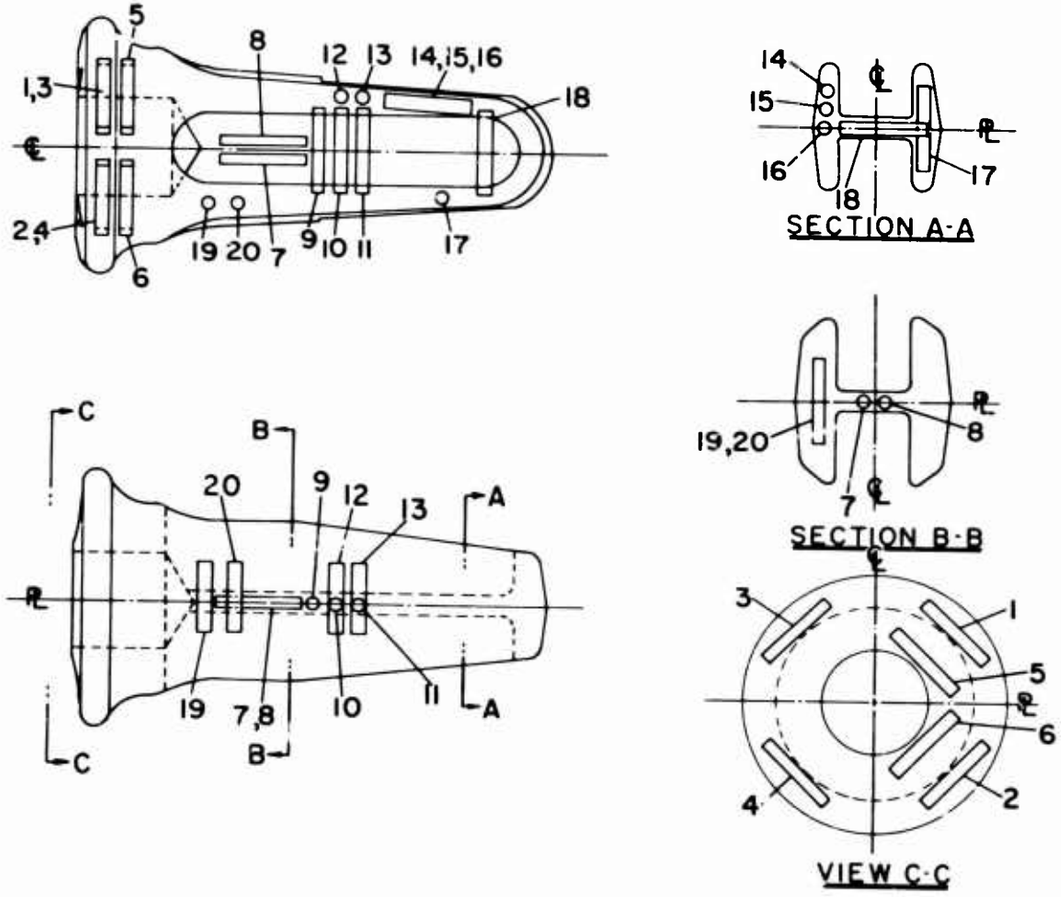

Figure 59. Location of Tensile Specimens in Sectioned Ti-6Al-6V-2Sn Cuff Forging.

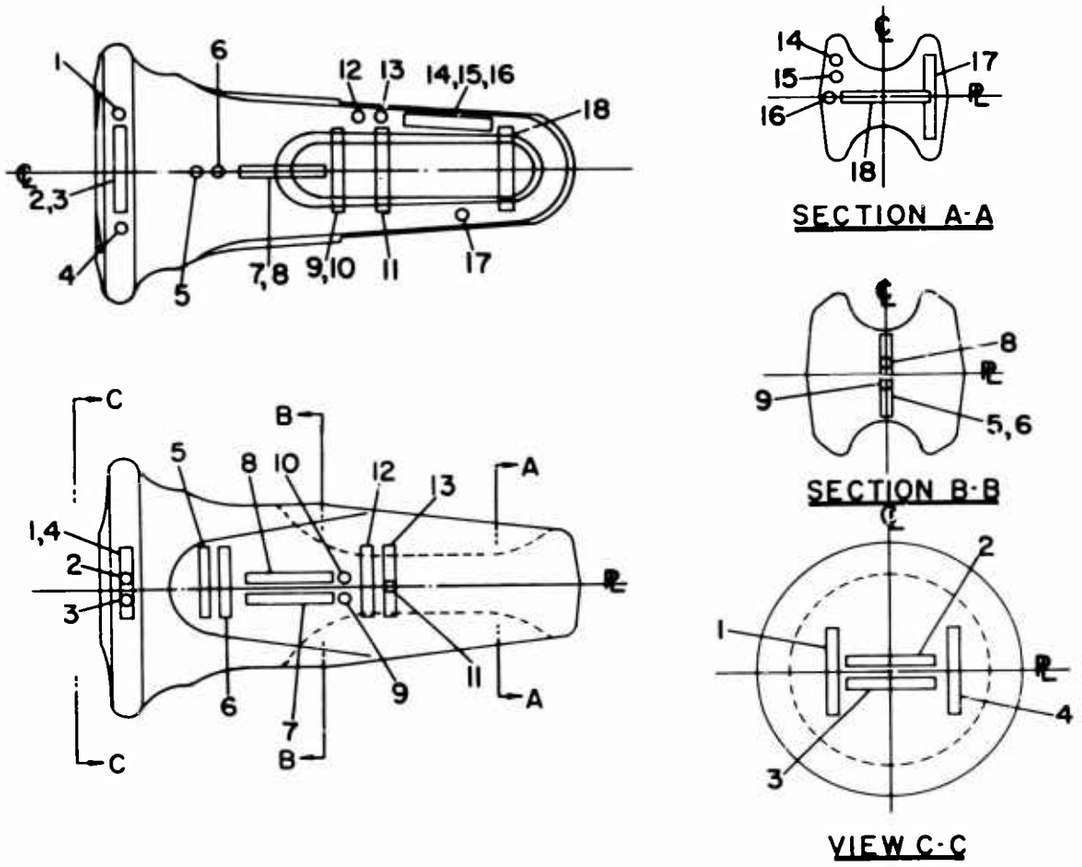

Figure 60. Location of Tensile Specimens in Sectioned Ti-13V-11Cr-3Al Cuff Forging.

All the Ti-6Al-6V-2Sn specimens from the sectioned forging exceeded the minimum desired ultimate tensile strength value of 165,000 psi. Some of the ultimate strength values from the sectioned Ti-13V-11Cr-3Al forging were slightly below the minimum desired 175,000-psi ultimate level, with the lowest value being 170,000 psi. In general, the tensile properties throughout all regions of the sectioned forgings of both alloys were uniform.

TABLE XXV

TENSILE TEST RESULTS
FOR SECTIONED Ti-6Al-6V-2Sn CUFF FORGING

Location	F_{tu} (ksi)	F_{ty} (ksi)	e (%)	R.A. (%)
1	173	160	12.0	33.2
2	176	162	14.0	43.1
3	176	164	12.0	40.1
4	172	160	12.0	40.1
5	174	160	8.0	20.3
6	173	160	7.0	17.4
7	173	162	7.5	18.1
8	173	162	7.5	16.0
9	178	166	9.0	25.1
10	178	166	9.5	26.6
11	174	166	10.0	31.1
12	172	160	8.5	25.1
13	172	159	8.5	29.2
14	170	160	10.5	25.9
15	170	160	13.0	31.9
16	173	162	11.0	31.9

TABLE XXV - Continued

Location	F_{tu} (ksi)	F_{ty} (ksi)	e (%)	R.A. (%)
17	177	164	10.0	28.6
18	178	166	11.0	32.7
19	170	156	8.5	23.7
20	175	160	7.0	18.1

TABLE XXVI

TENSILE TEST RESULTS
FOR SECTIONED Ti-13V-11Cr-3Al CUFF FORGING

Location	F_{tu} (ksi)	F_{ty} (ksi)	e (%)	R.A. (%)
1	175	166	4.0	4.5
2	172	161	4.0	6.2
3	173	160	3.5	6.2
4	176	165	5.0	6.2
5	174	163	4.0	4.7
6	176	165	4.0	5.5
7	170	161	4.5	7.0
8	176	166	4.0	8.6
9	182	171	5.0	7.0
10	174	164	4.5	9.3
11	182	171	4.5	7.0
12	174	164	4.5	10.0

TABLE XXVI - Continued

Location	F_{tu} (ksi)	F_{ty} (ksi)	e (%)	R.A. (%)
13	173	162	5.5	8.6
14	181	170	5.0	7.8
15	178	167	6.0	8.6
16	174	163	6.0	12.2
17	186	174	6.0	7.8
18	182	172	3.5	7.8

Photomicrographs indicating the structure obtained on the forgings in the hub and web area for both alloys are shown in Figures 61 and 62.

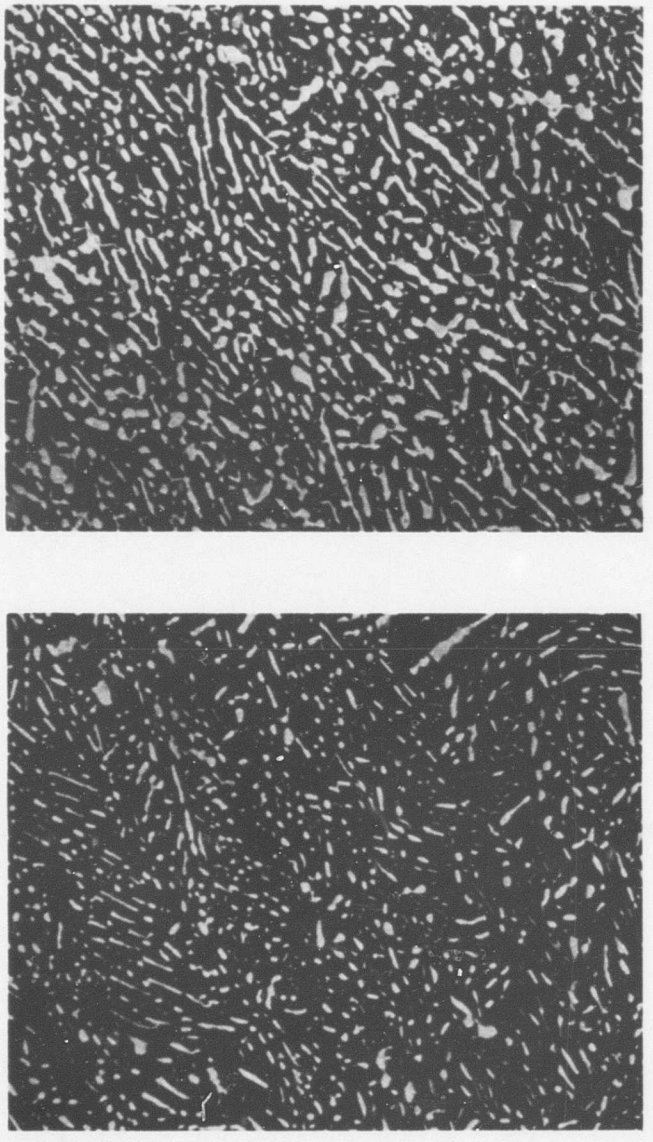

Figure 61. Photomicrograph of Ti-6Al-6V-2Sn Cuff Forging - Hub (Top) and Web (Bottom).

Note: Magnification 250X, Etchant HNO_3 + HF.

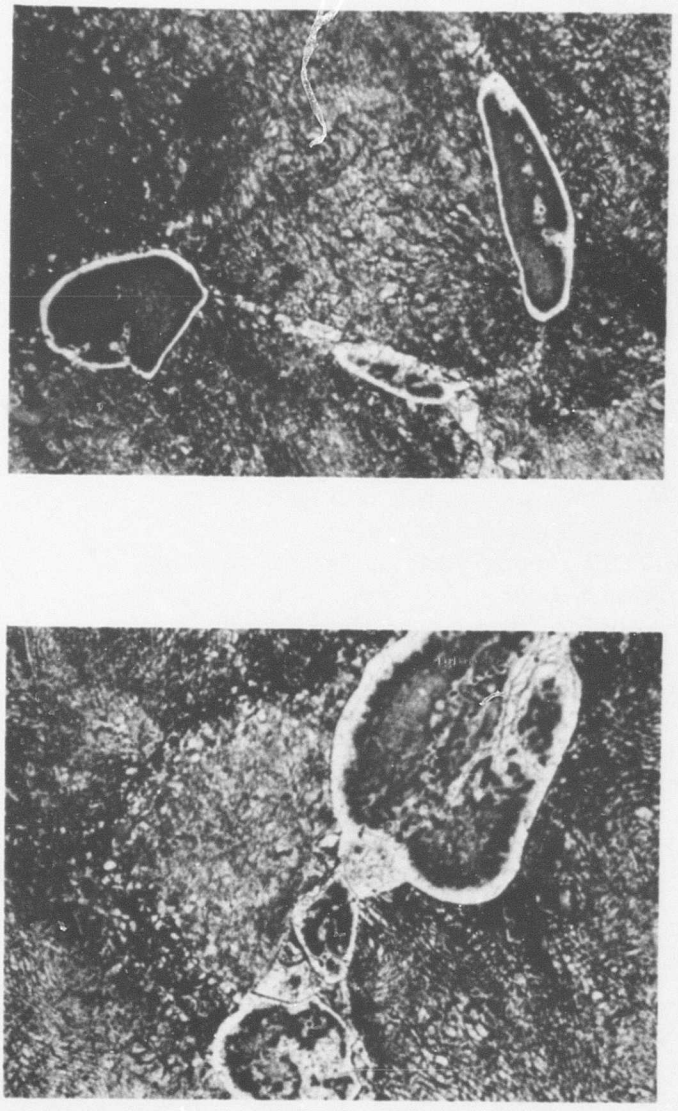

Figure 62. Photomicrograph of Ti-13V-11Cr-3Al Cuff Forging - Hub (Top) and Web (Bottom).

Note: Magnification 250X, Etchant H_3PO_4 + HF + $C_6H_{14}O_2$ (Electrolytic)

Unclassified

Security Classification

DOCUMENT CONTROL DATA - R&D

(Security classification of title, body of abstract and indexing annotation must be entered when the overall report is classified)

1. ORIGINATING ACTIVITY (Corporate author) Sikorsky Aircraft Division of United Aircraft Corporation Stratford, Connecticut	2a. REPORT SECURITY CLASSIFICATION Unclassified 2b. GROUP

3. REPORT TITLE

Evaluation of Two Titanium Forging Alloys

4. DESCRIPTIVE NOTES (Type of report and inclusive dates)

Final Report

5. AUTHOR(S) (Last name, first name, initial)

Matusovich, Charles J.

6. REPORT DATE	7a. TOTAL NO. OF PAGES	7b. NO. OF REFS
August 1967	89	5

8a. CONTRACT OR GRANT NO.	9a. ORIGINATOR'S REPORT NUMBER(S)
DA 44-177-AMC-256(T) b. PROJECT NO. c. Task 1F121401A14176 d.	USAAVLABS Technical Report 67-43 9b. OTHER REPORT NO(S) (Any other numbers that may be assigned this report) SER-50430

10. AVAILABILITY/LIMITATION NOTICES

Distribution of this document is unlimited.

11. SUPPLEMENTARY NOTES	12. SPONSORING MILITARY ACTIVITY
	US Army Aviation Materiel Laboratories Fort Eustis, Virginia

13. ABSTRACT

Two titanium forging alloys have been evaluated for aerospace applications: (a) Ti-6Al-6V-2Sn and (b) Ti-13V-11Cr-3Al (both solution heat-treated and aged). Both small-size specimens and full-size helicopter components were tested.

The small-size specimens were tested for resistance to fatigue crack initiation, resistance to fatigue crack propagation, and fracture toughness. Fatigue crack initiation tests included tension-tension tests both of unnotched specimens and of joints. Helicopter main rotor cuffs were evaluated in fatigue crack initiation and fatigue crack propagation tests with expanded holes and with reamed holes. The titanium alloy cuff test results were compared to those for Ti-6Al-4V (annealed) and 4340 steel (heat-treated to a 125-ksi minimum ultimate tensile strength) cuffs and to small-size specimen tests. Tensile test data, chemical analysis and forging parameters are also presented.

The crack initiation resistance of Ti-6Al-6V-2Sn was found to be superior to that of Ti-13V-11Cr-3Al. Axial tension-tension fatigue results showed 50% higher fatigue strengths for Ti-6Al-6V-2Sn than for Ti-13V-11Cr-3Al. Joint fatigue tests also showed higher strength values for the Ti-6Al-6V-2Sn alloy. Fracture toughness results were comparable for both alloys.

Joint fatigue test evaluations were made for reamed, shot peened, and expanded holes. The highest fatigue strength values were associated with specimens having expanded holes.

The Ti-6Al-6V-2Sn cuffs with both reamed and expanded cuff-to-spar attachment holes showed higher fatigue crack initiation strength values than those of the Ti-13V-11Cr-3Al.

The Ti-6Al-6V-2Sn cuffs showed higher resistance to crack propagation than Ti-13V-11Cr-3Al, with both reamed and expanded holes, and were comparable in resistance to crack propagation with 4340 steel and Ti-6Al-4V shot peened.

DD FORM 1 JAN 64 1473

Unclassified

Security Classification

Unclassified

Security Classification

14 KEY WORDS	LINK A		LINK B		LINK C	
	ROLE	WT	ROLE	WT	ROLE	WT

INSTRUCTIONS

1. ORIGINATING ACTIVITY: Enter the name and address of the contractor, subcontractor, grantee, Department of Defense activity or other organization *(corporate author)* issuing the report.

2a. REPORT SECURITY CLASSIFICATION: Enter the overall security classification of the report. Indicate whether "Restricted Data" is included. Marking is to be in accordance with appropriate security regulations.

2b. GROUP: Automatic downgrading is specified in DoD Directive 5200.10 and Armed Forces Industrial Manual. Enter the group number. Also, when applicable, show that optional markings have been used for Group 3 and Group 4 as authorized.

3. REPORT TITLE: Enter the complete report title in all capital letters. Titles in all cases should be unclassified. If a meaningful title cannot be selected without classification, show title classification in all capitals in parenthesis immediately following the title.

4. DESCRIPTIVE NOTES: If appropriate, enter the type of report, e.g., interim, progress, summary, annual, or final. Give the inclusive dates when a specific reporting period is covered.

5. AUTHOR(S): Enter the name(s) of author(s) as shown on or in the report. Enter last name, first name, middle initial. If military, show rank and branch of service. The name of the principal author is an absolute minimum requirement.

6. REPORT DATE: Enter the date of the report as day, month, year, or month, year. If more than one date appears on the report, use date of publication.

7a. TOTAL NUMBER OF PAGES: The total page count should follow normal pagination procedures, i.e., enter the number of pages containing information.

7b. NUMBER OF REFERENCES: Enter the total number of references cited in the report.

8a. CONTRACT OR GRANT NUMBER: If appropriate, enter the applicable number of the contract or grant under which the report was written.

8b, 8c, & 8d. PROJECT NUMBER: Enter the appropriate military department identification, such as project number, subproject number, system numbers, task number, etc.

9a. ORIGINATOR'S REPORT NUMBER(S): Enter the official report number by which the document will be identified and controlled by the originating activity. This number must be unique to this report.

9b. OTHER REPORT NUMBER(S): If the report has been assigned any other report numbers *(either by the originator or by the sponsor)*, also enter this number(s).

10. AVAILABILITY/LIMITATION NOTICES: Enter any limitations on further dissemination of the report, other than those imposed by security classification, using standard statements such as:

(1) "Qualified requesters may obtain copies of this report from DDC."

(2) "Foreign announcement and dissemination of this report by DDC is not authorized."

(3) "U. S. Government agencies may obtain copies of this report directly from DDC. Other qualified DDC users shall request through _____."

(4) "U. S. military agencies may obtain copies of this report directly from DDC. Other qualified users shall request through _____."

(5) "All distribution of this report is controlled. Qualified DDC users shall request through _____."

If the report has been furnished to the Office of Technical Services, Department of Commerce, for sale to the public, indicate this fact and enter the price, if known.

11. SUPPLEMENTARY NOTES: Use for additional explanatory notes.

12. SPONSORING MILITARY ACTIVITY: Enter the name of the departmental project office or laboratory sponsoring *(paying for)* the research and development. Include address.

13. ABSTRACT: Enter an abstract giving a brief and factual summary of the document indicative of the report, even though it may also appear elsewhere in the body of the technical report. If additional space is required, a continuation sheet shall be attached.

It is highly desirable that the abstract of classified reports be unclassified. Each paragraph of the abstract shall end with an indication of the military security classification of the information in the paragraph, represented as *(TS)*, *(S)*, *(C)*, or *(U)*.

There is no limitation on the length of the abstract. However the suggested length is from 150 to 225 words.

14. KEY WORDS: Key words are technically meaningful terms or short phrases that characterize a report and may be used as index entries for cataloging the report. Key words must be selected so that no security classification is required. Identifiers, such as equipment model designation, trade name, military project code name, geographic location, may be used as key words but will be followed by an indication of technical context. The assignment of links, rules, and weights is optional.

Unclassified

Security Classification

6038-67